

involved in the progression of chronic hepatitis (CH) and the development of liver cirrhosis (LC) and hepatocellular carcinoma (HCC) during the course of persistent HCV infection [3]. Thus, in this study we examined a possible correlation of serum concentrations of three chemokines, IL-8, monocyte chemoattractant protein-1 (MCP-1) or macrophage inflammatory protein-1 alpha (MIP-1 α), detected by a sandwich enzyme-linked immunosorbent assay (ELISA) system with the severity of chronic hepatitis C. The results suggest that IL-8 production is enhanced progressively with escalating severity of liver disease and the development of HCC.

2. Materials and methods

2.1. Patients

The patients in this study included 30 cases of CH, 29 cases of LC and 30 cases of HCC, who had been attending in Kanazawa University Hospital from April, 1999 to April, 2000. Participants eligible for the study were anti-HCV antibody negative, between 20 and 80 years of age. All the patients were positive for anti-HCV antibody and serum HCV RNA was quantitated with the Ampli-core HCV Monitor, version 2. In addition, 17 patients without chronic liver disease and also negative for anti-HCV antibody were enrolled as controls. All studied patients were negative for both hepatitis B surface antigen (HBsAg), HIV and alcoholic liver disease. In order to exclude the effects of inflammation other than liver diseases in our analyses, control subjects were selected with white blood cell (WBC) counts and C-reactive protein (CRP) values within normal range. There were significant differences in age, platelet count, alanine transaminase (ALT) activity and hepaplastin test (HPT) values among the four groups, i.e., CH, LC, HCC and control. These findings were considered to reflect differences in the pathological states among the groups (Table

1). This study was approved by the local ethics committee, and patients gave consent for the use of samples in these experiments.

2.2. Sandwich ELISA for IL-8, MCP-1 and MIP-1 α

Serum concentrations of IL-8, MCP-1 and MIP-1 α were determined by sandwich ELISA [4,5]. Each well in 96-well plates was coated with 100 μ l of either anti-IL-8, anti-MCP-1 or anti-MIP-1 α monoclonal antibody overnight at 4 °C. The wells were then treated with blocking solution (1% BSA-PBS) for 1 h at 37 °C. Serum samples were diluted with Tween-PBS containing 0.5% BSA and 100 μ l of the samples were added to the wells and incubated at overnight 4 °C. Then, 100 μ l of rabbit polyclonal antibodies against each of the chemokines (1 μ g/ml) was added to the wells and the plates were incubated for 2 h at 37 °C. Thereafter, alkaline phosphatase conjugated anti-rabbit IgG was added to the wells and the plates were incubated for 2 h at 37 °C. Finally, 1 M diethanolamine (pH 9.8) containing 1 mg/ml *p*-nitrophenyl phosphate was added and the optical density of each well at 405 nm was measured using a microplate reader.

2.3. Criteria for clinical and pathological study

Serum chemokine concentrations were compared with the severity of chronic hepatitis C, macroscopic stages of HCC and the survival periods of the patients. Pathological classification of HCC was performed using general criteria for the clinical and pathological study of primary HCC [6].

2.4. Immunohistochemistry

Paraffin embedded sections of liver tissues were immunostained with mouse monoclonal IgG antibody against IL-8 at dilutions of 1:20 as described previously [7,8]. Then, horseradish peroxidase-labeled anti-mouse IgG

Table 1
Clinical characteristics of patients studied

| | CH (n = 30) | LC (n = 29) | HCC (n = 30) | Control (n = 17) | P |
|--------------------------------|------------------|-----------------|------------------|------------------|-----------------|
| Age (year) | 48.8 \pm 11.1 | 58.0 \pm 8.4 | 66.6 \pm 6.0 | 58.6 \pm 15.6 | <0.01* |
| Sex (M/F) | 23/7 | 18/11 | 18/12 | 12/5 | NS ^a |
| WBC (/ μ l) | 5050 \pm 1560 | 4360 \pm 1470 | 3940 \pm 1630 | 5760 \pm 1850 | NS* |
| Plt ($\times 10^4$ / μ l) | 17.3 \pm 5.1 | 9.9 \pm 4.7 | 10.3 \pm 5.1 | 20.7 \pm 6.8 | <0.01* |
| CRP (mg/dl) | 0.12 \pm 0.14 | 0.20 \pm 0.45 | 0.80 \pm 1.60 | 0.30 \pm 0.56 | NS* |
| ALT (IU/l) | 100.0 \pm 82.8 | 76.6 \pm 52.8 | 83.7 \pm 104.6 | 25.0 \pm 19.0 | <0.05* |
| HPT (%) | 79.8 \pm 11.4 | 70.1 \pm 15.6 | 60.3 \pm 14.6 | 92.5 \pm 32.8 | <0.01* |

Note. Results are expressed as means \pm SD.

Abbreviations: WBC, white blood cell; Plt, platelet; CRP, C-reactive protein; ALT, alanine transaminase; HPT, hepaplastin test; CH, chronic hepatitis; LC, liver cirrhosis; HCC, hepatocellular carcinoma; NS, not significant.

^a Fisher's exact test.

* Kruskal–Wallis test.

(Vector Laboratories, Inc., Burlingame, CA), was added and incubated. Immunocomplexes were detected with diaminobenzidine (Sigma Chemical Co, St. Louis, MO).

2.5. Statistical analysis

Differences between groups were analyzed for statistical significance using one-way ANOVA and the Mann–Whitney *U* test. Qualitative variables were compared by means of Fisher's exact test. Factors significantly associated with the progression of liver disease were determined by multivariate logistic regression analysis. All tests were two-tailed, and a *P*-value of <0.05 was considered statistically significant.

3. Results

3.1. Serum chemokine levels in patients with chronic hepatitis C

Correlation of serum chemokine levels with the severity of chronic liver disease was examined in patients with chronic hepatitis C (Fig. 1). The detection limits of our ELISA systems for IL-8, MCP-1 and MIP-1 α were 10, 40 and 10 pg/ml, respectively. Serum IL-8 levels were elevated progressively as the disease severity increased: control group, 17.43 ± 1.11 pg/ml; CH group, 18.75 ± 2.32 pg/ml; LC group, 32.12 ± 3.80 pg/ml; and HCC group 49.13 ± 11.03 pg/ml ($P < 0.01$). In contrast, there was no correlation between serum MCP-1 concentrations and the severity of chronic hepatitis C: control group, 209.56 ± 26.33 pg/ml; CH group, 219.22 ± 54.55 pg/ml; LC group, 192.75 ± 59.52 pg/ml; and HCC group, 302.67 ± 44.52 pg/ml ($P = 0.057$). In addition, serum MIP-1 α levels did not correlate with disease severity: control group, 21.26 ± 9.26 pg/ml; CH group, 27.83 ± 14.57 pg/ml; LC group, 17.99 ± 6.63 pg/ml; and HCC group, 28.37 ± 7.95 pg/ml ($P = 0.051$). The data suggest that IL-8 production may be induced in the process of disease progression in chronic HCV infection.

3.2. Serum IL-8 levels in patients with HCC classified according to the severity liver damage

Since serum IL-8 levels were high in the HCC group, as shown in Fig. 1, we examined whether there were any differences in serum IL-8 concentrations among patients with varying stages of HCC. Namely, we evaluated the correlation between serum IL-8 levels and the degree of liver damage, which reflects the hepatic reserve in HCC patients: liver damage A, 29.98 ± 6.59 pg/ml; liver damage B, 58.80 ± 35.37 pg/ml; and liver damage C, 81.54 ± 25.11 pg/ml. There was a tendency for increased values with the progression of liver damage, although this effect was not significant.

3.3. Serum IL-8 levels in patients with HCC classified according to macroscopic staging

A correlation between the macroscopic staging of HCC and serum IL-8 levels was examined (Fig. 2): stage I, 33.10 ± 10.79 pg/ml; stage II, 46.12 ± 20.93 pg/ml; stage III, 16.27 ± 5.36 pg/ml; stage IV-A, 41.25 ± 12.86 pg/ml; and stage IV-B, 153.20 ± 47.22 pg/ml. Serum IL-8 values of patients in stage IV-B were significantly higher than those of patients in other stages. Thus, patients with advanced HCC accompanying remote metastasis (stage IV-B) were found to show elevated IL-8 levels, compared with patients without remote metastasis. In addition, we observed the elevation of IL-8 following the detection of HCC bone metastasis in two cases of stage IV-B whose serial samples were preserved (Fig. 3), suggesting that serum levels of IL-8 may directly reflect the onset of HCC remote metastasis.

3.4. Serum IL-8 levels in patients with HCC classified according to survival periods

When a correlation between serum IL-8 levels and the survival periods of patients with HCC was evaluated, patients with poor prognosis gave significantly higher val-

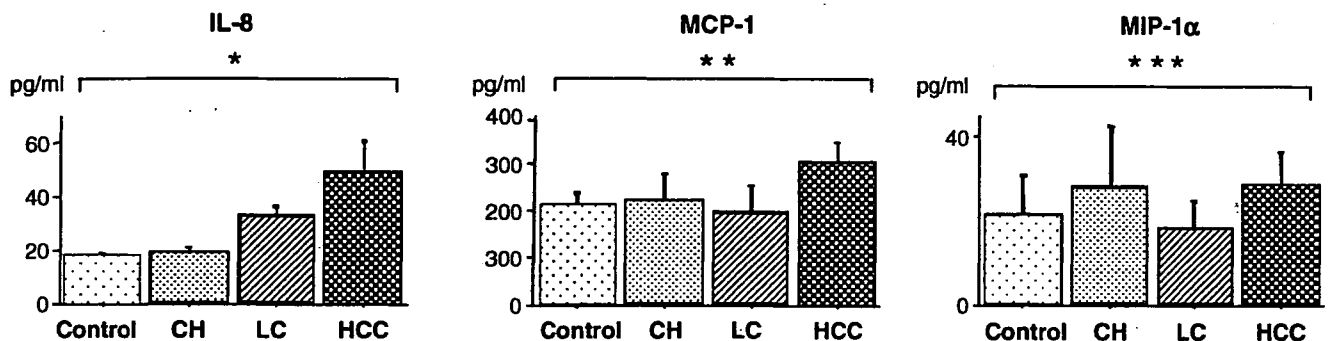


Fig. 1. Serum chemokine levels in patients with chronic hepatitis C, including 30 cases of chronic hepatitis (CH), 29 cases of liver cirrhosis (LC), 30 cases of hepatocellular carcinoma (HCC) and 17 controls. Serum IL-8 levels were elevated with the progression of disease: **F*: 4.63, $P < 0.01$ when compared by analysis of ANOVA. Serum MCP-1 and MIP-1 α concentrations were not correlated with disease severity: ***F*: 0.99, $P = 0.057$; ****F*: 0.27, $P = 0.051$, respectively.

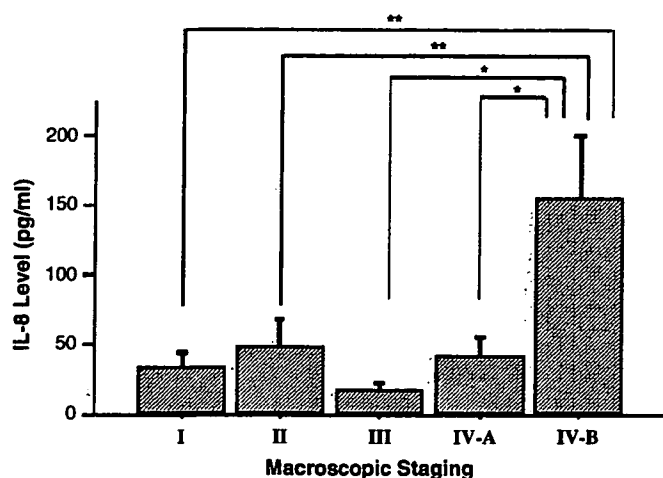


Fig. 2. Serum IL-8 levels in patients with HCC classified according to macroscopic staging. Stage I ($n = 3$) of macroscopic stage by the Liver Cancer Study Group of Japan; T1, N0, M0. Stage II ($n = 4$); T2, N0, M0. Stage III ($n = 7$); T3, N0, M0 or T1-3, N1, M0. Stage IV-A ($n = 12$); T4, N0-1, M0. Stage IV-B ($n = 4$); T1-4, N0-1, M1. In the HCC patients, IL-8 concentrations were positively correlated with macroscopic stages. $F: 5.51$, $P < 0.01$ when compared by analysis of ANOVA. $*P < 0.01$ when compared by Mann-Whitney U test. $**P < 0.05$ when compared by Mann-Whitney U test.

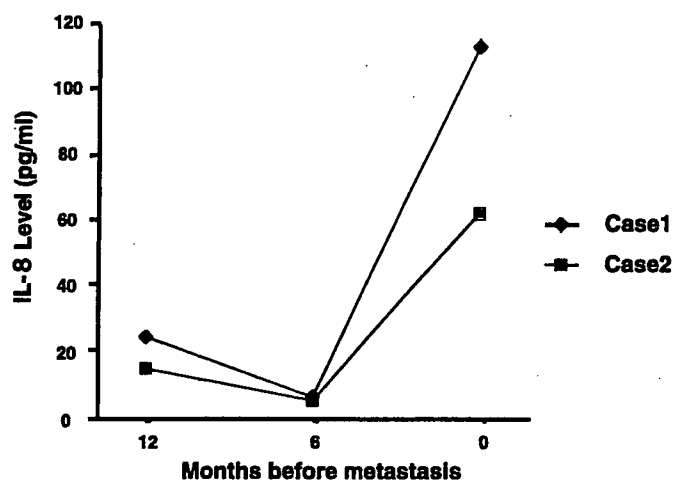


Fig. 3. Course of serum IL-8 levels in patients with HCC accompanying remote metastasis. Both cases 1 and 2 show the elevation of IL-8 following the detection of HCC bone metastasis.

ues (Fig. 4): over a 1-year survival period, 22.05 ± 5.90 pg/ml; over 3 months but less than 1 year, 64.34 ± 19.78 pg/ml; and less than 3 months, 132.72 ± 54.16 pg/ml. Furthermore, we performed multivariate logistic regression analysis between the prognosis of patients with HCC, and their ages, platelet counts, prothrombin times (PT), albumin levels, alpha-fetoprotein (AFP), IL-8 levels and the presence or absence of ascites (Table 2). The results indicated that AFP was not a factor that determined the prognosis, but IL-8 concentration was found to be an independent risk factor for a poor prognosis, as well as platelet count and serum albumin concentration elevated.

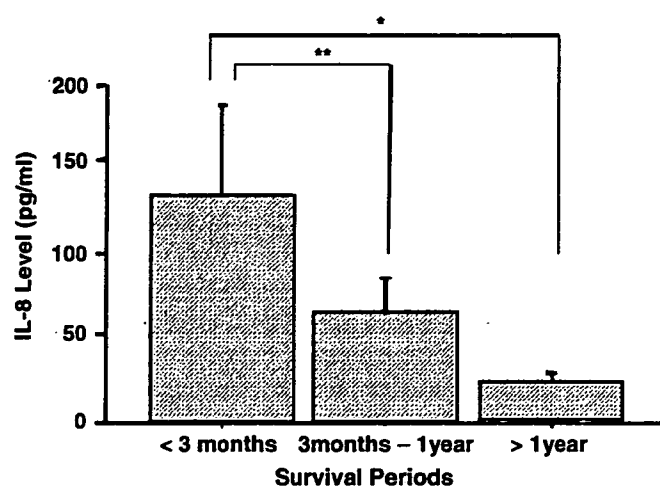


Fig. 4. Serum IL-8 levels in patients with HCC classified according to survival periods, <3 months ($n = 3$), 3 months–1 year ($n = 12$) and >1 year ($n = 16$). IL-8 concentrations were inversely correlated with the length of the survival periods. $F: 6.40$, $P < 0.01$ when compared by analysis of ANOVA. $*P < 0.01$ when compared by Mann-Whitney U test. $**P < 0.05$ when compared by Mann-Whitney U test.

3.5. IL-8 expression in liver cells

To identify IL-8 producing cells in the liver, an immunohistochemical analysis of liver tissues was performed. IL-8 was strongly stained in the cytoplasm of HCC cells, was weakly stained in the cytoplasm of some hepatocytes in LC, and was undetectable in hepatocytes from control tissue (Fig. 5). The data indicated that IL-8 is produced upon the malignant transformation of hepatocytes.

4. Discussion

The current study demonstrates that of the three chemokines, IL-8, MCP-1 and MIP-1 α , determined by ELISA in patients with chronic hepatitis C, serum concentrations of IL-8 alone were increased, correlating with the progression of liver disease. Notably, the levels of IL-8 were significantly increased in patients with advanced HCC with remote metastasis and IL-8 levels were elevated in patients with poor prognoses. Interestingly, immunohistochemical analysis showed that IL-8 was detectable mainly in the cytoplasm of HCC cells. These findings suggest that the expression of IL-8 may be augmented upon the malignant transformation of hepatocytes during the course of chronic HCV infection.

IL-8 is known to be closely associated with pathological states of CH through the activation of inflammatory cells such as granulocytes or T lymphocytes. The levels of IL-8 were elevated in

Table 2
Characteristics of patients with HCC classified according to survival periods

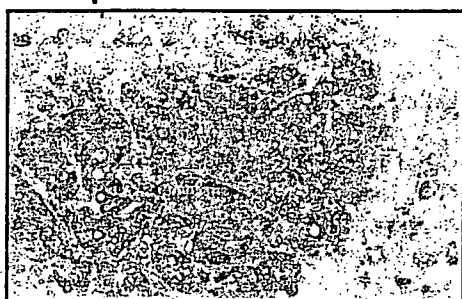
| | >3 months (n = 3) | 3 months–1 year (n = 12) | <1 year (n = 16) | Logistic regression | |
|----------------------------|-------------------|--------------------------|------------------|------------------------|--------|
| | | | | Regression coefficient | P* |
| Age (year) | 68.7 ± 3.8 | 68.3 ± 6.0 | 65.0 ± 6.3 | 3.067 | 0.2157 |
| Plt (×10 ⁴ /μl) | 9.3 ± 3.7 | 11.4 ± 6.1 | 9.6 ± 4.7 | 6.737 | 0.0344 |
| PT (s) | 14.3 ± 1.7 | 12.5 ± 1.5 | 12.2 ± 1.5 | 1.862 | 0.3942 |
| Alb (mg/dl) | 3.4 ± 1.0 | 3.4 ± 0.5 | 3.8 ± 0.9 | 9.013 | 0.0110 |
| AFP (ng/ml) | 57600 ± 57600 | 29300 ± 28900 | 252 ± 137 | 1.593 | 0.4509 |
| IL-8 (pg/ml) | 132.7 ± 54.2 | 64.3 ± 21.6 | 22.1 ± 5.9 | 10.196 | 0.0061 |
| Ascites | 2/3 | 2/12 | 2/16 | 0.003 | 0.9984 |

Note. Results are expressed as means ± SD.

Abbreviations: Plt, Platelet; PT, prothrombin time; Alb, albumin; AFP, alpha-fetoprotein; IL-8, interleukin-8.

* Kruskal–Wallis test.

A Hepatocellular Carcinoma



B Cirrhotic Liver



Fig. 5. Immunohistochemical analysis of liver tissues stained with the anti-IL-8 antibody. Five surgically resected HCC tissues were examined, in three cases IL-8 was strongly stained in the cytoplasm of HCC cells. A representative case of HCC stage II was shown in (A), whose serum IL-8 level was 28 pg/ml. IL-8 was weakly expressed in the cytoplasm of some hepatocytes in the cirrhotic liver (B) and was undetectable in hepatocytes of the control tissues (not shown). Original magnification 200×.

patients with acute and chronic liver damages, e.g., viral hepatitis, autoimmune hepatitis or alcohol-induced liver dysfunction [9–14]. Moreover, it has been reported that there is a correlation between IL-8 levels and the severity of liver disorders, including HCV infection [15–18]. Recently it has also been reported that the core and NS5A proteins of HCV induce the expression of the IL-8 gene [3], and that serum IL-8 levels in chronic hepatitis C patients are

associated with resistance to interferon treatment [19], suggesting that IL-8 plays an important role in the maintenance of persistent infection with HCV. In the current study, serum IL-8 levels increased as the disease progressed from CH to LC and further to HCC, suggesting that the increase may be due not only to immune response against persistent HCV infection but to the development of HCC.

There has been no report, to our knowledge, investigating the possible correlation between serum MCP-1 or MIP-1α level and the pathology of chronic liver disease. The present results did not indicate a significant correlation between them. Therefore, we conclude that persistent HCV infection may not increase serum MCP-1 or MIP-1α levels.

Among the many chemokines, IL-8 level has been reported to show a tendency to increase during the progression of cancers of the stomach [20], pancreas [21], lung [22] and prostate [23]. In patients with HCC, IL-8 was shown to be expressed in the cytoplasm of hepatoma cells and in vascular endothelial cells of tumors [7,24,25], suggesting that the angiogenetic activity of IL-8 may contribute to the growth of HCC. In addition, we have observed that neither of the two IL-8 receptors, CXC chemokine receptor (CXCR) 1 or CXCR2, is detectable in HCC cell lines or tissues [5], suggesting that the growth promotion of HCC cells by IL-8 may be an indirect effect. IL-8 has the capacity to recruit various inflammatory cells that eventually produce proinflammatory cytokines including IL-1. Recently, we found that IL-1 enhances the production of CC chemokine ligand 3 (CCL3) which may interact with the CC chemokine receptor (CCR) 1 on HCC cells and contribute to tumor pro-

gression [5]. Moreover IL-8 levels were reported to be correlated with the growth of breast cancer cells having a high metastatic activity [26]. In line with these observations, our study similarly indicated that serum IL-8 levels were highly elevated in patients with HCC accompanied by remote metastasis (stage IV-B). Furthermore, we observed that serum IL-8 values rose following the detection of HCC bone metastasis in two cases. These findings suggest that IL-8 may promote the attachment and growth of cancer cells at extrahepatic sites. Moreover, IL-8 levels in cervical cancer tissues were shown to be correlated with the prognosis of patients [27]. Otherwise, IL-8 levels can simply correlate with overall tumor burden at advanced stages of HCC. Consistent with these observations, our study also showed that serum IL-8 levels increased significantly in patients with poor prognoses and whose survival periods were less than 1 year, as compared with patients with better prognoses. When we performed multivariate regression analyses of possible prognosis factors, IL-8, as well as platelet counts and albumin levels, was found to be a significant factor. These findings suggest that serum IL-8 levels can be a marker predicting the prognosis of patients with HCC.

This study indicates that IL-8 may be involved in the progression of chronic hepatitis C and the development of HCC. There is a report indicating the significant correlations of IL-8 levels with tumor size and disease stage in chronic hepatitis B as well [28], suggesting that IL-8 may be a useful biological marker of HCC invasiveness and a prognostic factor for HCC patients. The molecular biological mechanisms explaining these findings remain to be clarified in the future by using HCC cell lines or animal models.

Acknowledgments

The authors express our gratitude to Dr. Yasukazu Ohmoto (Cellular Technology Institute, Ohtsuka Pharmaceutical Ltd.) for providing us with an ELISA kit for human MIP-1 α . We thank Ms. Akemi Nakano for her excellent technical assistance.

References

- [1] F. Melchers, A.G. Rolink, C. Schaniel, The role of chemokines in regulating cell migration during humoral immune responses, *Cell* 99 (1999) 351–354.
- [2] J.J. Campbell, E.C. Butcher, Chemokines in tissue-specific and microenvironment-specific lymphocyte homing, *Curr. Opin. Immunol.* 12 (2000) 336–341.
- [3] S.J. Polyak, K.S. Khabar, D.M. Paschal, et al., Hepatitis C virus nonstructural 5 A protein induces interleukin-8, leading to partial inhibition of the interferon-induced antiviral response, *J. Virol.* 75 (2001) 6095–6106.
- [4] H. Yokoyama, T. Wada, K. Furuichi, et al., Urinary levels of chemokines (MCAF/MCP-1, IL-8) reflect distinct disease activities and phases human IgA nephropathy, *J. Leukoc. Biol.* 63 (1998) 493–499.
- [5] P. Lu, Y. Nakamoto, Y. Memoto-Sasaki, et al., Potential interaction between CCR1 and its ligand, CCL3, induced by Endogenously produced interleukin-1 in human. hepatoma, *Am. J. Pathol.* 162 (2003) 1249–1258.
- [6] Liver cancer study group of Japan. The general rules for the clinical and pathological study of primary liver cancer, *Jpn. J. Surg.* 19 (1989) 98–129.
- [7] A. Iguchi, I. Kitajima, M. Yamakuchi, et al., PEA3 and AP-1 are required for constitutive IL-8 gene expression in hepatoma cells, *Biochem. Biophys. Res. Commun.* 279 (2000) 166–179.
- [8] Y. Takahashi, T. Kasahara, T. Sawai, et al., The participation of IL-8 in the synovial lesion at an early stage of rheumatoid arthritis, *J. Exp. Med.* 188 (1999) 75–87.
- [9] D.B. Hill, Increased plasma interleukin-8 concentration in alcoholic hepatitis, *Hepatology* 18 (1993) 576–580.
- [10] N. Sheron, G. Bird, J. Koskinas, et al., Circulation and tissue levels of the neutrophil chemotaxin interleukin-8 are elevated in severe acute alcoholic hepatitis, and tissue levels correlate with neutrophil infiltration, *Hepatology* 18 (1993) 41–46.
- [11] J. Napoli, G.A. Bishop, G.W. McCaughan, Increased intrahepatic messenger RNA expression of interleukin 2, 6, and 8 in human cirrhosis, *Gastroenterology* 107 (1994) 789–798.
- [12] J. Maggiore, F. Benedetti, M. Massa, P. Pignatti, A. Martini, Circulating levels of interleukin-6, interleukin-8, and tumor necrosis factor- α in children with autoimmune hepatitis, *J. Pediatr. Gastroenterol. Nutr.* 20 (1995) 23–27.
- [13] A. Al-Wabel, B. al-Knawy, S. Raziuddin, Interleukin-8 and granulocytemacrophage colony-stimulating factor secretion in hepatocellular carcinoma and viral chronic active hepatitis, *Clin. Immunol. Immunopathol.* 74 (1995) 231–235.
- [14] T. Masumoto, K. Ohkubo, K. Yamamoto, et al., Serum IL-8 levels and localization IL-8 in liver from patients with chronic viral hepatitis, *Hepatogastroenterology* 45 (1998) 630–634.
- [15] P.J. Scheuer, P. Ashrafzadeh, S. Sherlok, D. Brown, G.M. Dusheiko, The pathology of hepatitis C, *Hepatology* 15 (1992) 567–571.
- [16] G. Kaplanski, C. Franarier, M.J. Payan, P. Bongerd, J.M. Durand, Increased levels of soluble adhesion molecules in the serum of patients with hepatitis C, *Dig. Dis. Sci.* 42 (1997) 2277–2284.
- [17] K. Shimoda, M.A. Begum, K. Shibuta, M. Mori, H.L. Bonkovsky, B.F. Banner, G.F. Barnard, Interleukin-8 and hIRH(SDFI- α /PBSF) mRNA expression and histological activity index in patients with chronic hepatitis C, *Hepatology* 28 (1998) 108–115.
- [18] M.G. Neuman, J.P. Benhamou, I.M. Malkiewicz, et al., Cytokines as predictors for sustained response and as

- markers for immunomodulation in patients with chronic hepatitis C, *Clin. Biochem.* 34 (2001) 173–182.
- [19] S.J. Polk, K.S.A. Khabar, M. Rezeiq, D.R. Gretch, Elevated levels of interleukin-8 in serum are associated with hepatitis C virus infection and resistance to interferon therapy, *J. Virol.* 75 (2001) 6209–6211.
- [20] Y. Kitadai, K. Haruma, N. Mukaida, et al., Regulation of Disease-Progression genes in human gastric carcinoma cell by interleukin 8, *Clin. Cancer Res.* 6 (2000) 2735–2740.
- [21] M. Miyamoto, Y. Shimizu, K. Okada, Y. Kashi, K. Higuchi, A. Watanabe, Effect of interleukin-8 on producing of tumor-associated substances and autocrine growth of human liver and pancreatic cancer cells, *Cancer Immunol. Immunother.* 47 (1998) 47–57.
- [22] R.M. Striter, P.J. Polverini, D.A. Arenberg, et al., Role of C-X-C chemokines as regulators of angiogenesis in lung cancer, *J. Leukoc. Biol.* 57 (1995) 752–762.
- [23] G.F. Greene, Y. Kitadai, C.A. Pettaway, A.C. Von Eschenbach, C.D. Bucana, I.J. Fidler, Correlation of metastasis-related gene expression with metastatic potential in human prostate carcinoma cells implanted in nude mice using an in situ messenger RNA hybridization technique, *Am. J. Pathol.* 150 (1997) 1571–1582.
- [24] K.F. Yoong, S.C. Afford, R. Jones, et al., Expression and function of CXC and CC chemokines in human malignant liver tumor: a role for human monokine induced by gamma-interferon in lymphocyte recruitment to hepatocellular carcinoma, *Hepatology* 30 (1999) 100–111.
- [25] J. Akiba, H. Yano, S. Ogasawara, K. Higake, M. Kojiro, Expression and function of interleukin-8 in human hepatocellular carcinoma, *Int. J. Oncol.* 18 (2000) 257–264.
- [26] E.J. De Larco, R.K.B. Wuertz, A.K. Rosner, et al., A potential role for interleukin-8 in the metastatic phenotype of breast carcinoma cells, *Am. J. Pathol.* 158 (2001) 639–646.
- [27] J. Fujimoto, H. Sakaguchi, I. Aoki, T. Tamaya, Clinical implication of expression of interleukin 8 related to angiogenesis in uterine cervical cancer, *Cancer Res.* 60 (2000) 2632–2635.
- [28] Y. Ren, R.T. Poon, H.T. Tsui, et al., Interleukin-8 levels in Patients with Hepatocellular carcinoma: correlation with Clinicopathological features and prognosis, *Clin. Cancer Res.* 9 (2003) 5996–6001.

Prolonged, NK Cell-Mediated Antitumor Effects of Suicide Gene Therapy Combined with Monocyte Chemoattractant Protein-1 against Hepatocellular Carcinoma

Tomoya Tsuchiyama,* Yasunari Nakamoto,* Yoshio Sakai,* Yohei Marukawa,* Masaaki Kitahara,* Naofumi Mukaida,[†] and Shuichi Kaneko^{1*}

Tumor recurrence rates remain high after curative treatments for hepatocellular carcinoma (HCC). Immunomodulatory agents, including chemokines, are believed to enhance the antitumor effects of tumor cell apoptosis induced by suicide gene therapy. We therefore evaluated the immunomodulatory effects of a bicistronic recombinant adenovirus vector (rAd) expressing both HSV thymidine kinase and MCP-1 on HCC cells. Using an athymic nude mouse model (BALB/c-*nu/nu*), primary s.c. tumors (HuH7; human HCC cells) were completely eradicated by rAd followed by treatment with ganciclovir. The same animals were subsequently rechallenged with HCC cells, tumor development was monitored, and the recruitment or activation of NK cells was analyzed immunohistochemically or by measuring IFN- γ mRNA expression. Tumor growth was markedly suppressed as compared with that in mice treated with a rAd expressing the HSV thymidine kinase gene alone ($p < 0.001$). Suppression of tumor growth was associated with the elevation of serum IL-12 and IL-18. During suppression, NK cells were recruited exclusively, and Th1 cytokine gene expression was enhanced in tumor tissues. The antitumor activity, however, was abolished either when the NK cells were inactivated with anti-asialo GM1 Ab or when anti-IL-12 and anti-IL-18 Abs were administered. These results indicate that suicide gene therapy, together with delivery of MCP-1, eradicates HCC cells and exerts prolonged NK cell-mediated antitumor effects in a model of HCC, suggesting a plausible strategy to prevent tumor recurrence. *The Journal of Immunology*, 2007, 178: 574–583.

Despite curative treatments including surgical resection and liver transplantation for hepatocellular carcinoma (HCC),² tumor recurrence rates remain high, probably because of insufficient therapeutic effects and the multicentric development of HCC in cirrhotic liver (1–3). Although nonsurgical treatments of HCC such as radiofrequency ablation, transcatheter arterial embolizations, and transcatheter arterial chemotherapy induce apoptosis of HCC cells, these treatments do not enhance antitumoral immunity sufficiently. Therefore, gene therapy aimed at enhancing antitumor immune responses may be a promising approach to induce sufficient inhibitory effects for the prevention of tumor recurrence.

Although killing tumor cells with cytotoxic genes such as suicide gene/prodrug systems consisting of HSV thymidine kinase (HSV-tk) and ganciclovir (GCV) may lead to the genera-

tion of effective immunity (4, 5), cell killing alone is insufficient to increase many antitumor responses (6–8). Recently, however, coexpression of HSV-tk and chemokines was found to increase tumor immunity in animal models in which neither HSV-tk nor chemokine expression alone was sufficient (9). In addition, we previously demonstrated that, at the local treatment site, the antitumor effects of the HSV-tk/GCV system were enhanced by codelivery of MCP-1, a member of the CC chemokine family (8, 10). MCP-1 has been shown to stimulate the cytotoxic activity of monocytes, enhance the expression of adhesion molecules such as CD11b and CD11c, and induce the cytotoxic and migratory activities of NK cells (11–14). Moreover, transfection of the MCP-1 into human lung adenocarcinoma cells inhibited the formation of metastases, presumably via the activation of NK cells (15). It was recently reported that NK cells can mediate long-lived, Ag-specific adaptive recall responses independently of B cells and T cells (16). These observations suggest that MCP-1 can induce specific tumor immunity by enhancing NK cell functions even in this system.

Thus, we evaluated the long-term systemic immunomodulatory effects of a bicistronic recombinant adenovirus vector (rAd) expressing both HSV-tk and MCP-1 (Ad-tk-MCP1). After the primary s.c. HCC tumors in athymic nude mice were eradicated by using Ad-tk-MCP1, the same HCC cells were injected into another site of the same mice to prove the presence of NK cell-mediated, long-term immunity. Moreover, we explored whether innate immune responses induced by NK cells were involved in these procedures. In this study, we provide definitive evidence to indicate that codelivery of a suicide gene and MCP-1 exerts prolonged NK cell-mediated antitumor effects in this model, suggesting a plausible strategy to prevent HCC recurrence.

*Department of Gastroenterology, Graduate School of Medical Science and [†]Division of Molecular Bioregulation, Cancer Research Institute, Kanazawa University, Kanazawa, Japan

Received for publication October 27, 2005. Accepted for publication October 13, 2006.

The costs of publication of this article were defrayed in part by the payment of page charges. This article must therefore be hereby marked *advertisement* in accordance with 18 U.S.C. Section 1734 solely to indicate this fact.

¹ Address correspondence and reprint requests to Dr. Shuichi Kaneko, Department of Gastroenterology, Graduate School of Medical Science, Kanazawa University, 13-1 Takara-machi, Kanazawa 920-8641, Japan. E-mail address: skaneko@medf.m.kanazawa-u.ac.jp

² Abbreviations used in this paper: HCC, hepatocellular carcinoma; AGMI, asialo GM1; BNL, BNL IME A.7R.1 HCC cell line; DC, dendritic cell; GCV, ganciclovir; HSV-tk, HSV thymidine kinase; MMC, mitomycin C; MOI, multiplicity of infection; rAd, recombinant adenovirus vector; Ad-tk, rAd expressing HSV-tk; Ad-tk-MCP1, rAd expressing both HSV-tk and MCP-1; Ad-MCP1, rAd expressing MCP-1; Ad-lacZ, rAd expressing lacZ; TCID₅₀, 50% tissue culture infectious dose.

Copyright © 2006 by The American Association of Immunologists, Inc. 0022-1767/06/\$2.00

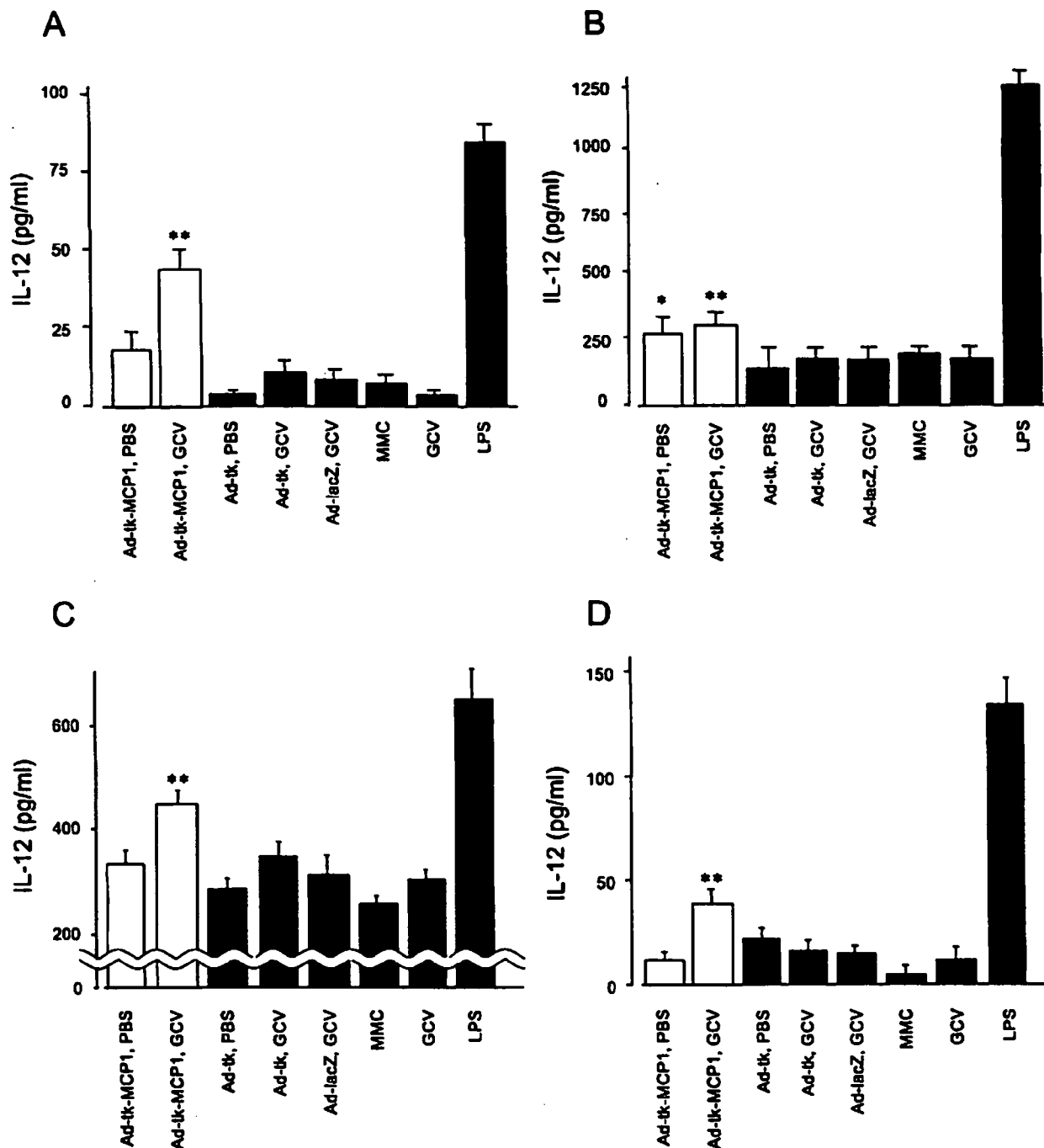


FIGURE 1. IL-12 production by monocytes and DCs cocultured with apoptotic or nonapoptotic HCC cells infected with rAds in vitro. HuH7 cells were infected with Ad-tk-MCP1, Ad-tk, and Ad-lacZ at an MOI of 5 for 24 h. Aliquots of 10^5 mouse (A) and human (C) monocytes or 10^5 mouse (B) and human (D) DCs were cocultured with 10^5 rAd- or MMC-treated HuH7 cells and treated with or without GCV for two days, and the concentrations of IL-12 in the medium were evaluated using an immunoassay. Each value is the mean \pm SE of triplicate experiments. *, $p < 0.05$ compared to Ad-tk with PBS (Ad-tk, PBS); **, $p < 0.05$ compared to Ad-tk with GCV (Ad-tk, GCV) by the Mann-Whitney *U* test.

Materials and Methods

Recombinant adenoviruses

The bicistronic Ad-tk-MCP1 (10), which harbors the HSV-tk gene and the human MCP-1 gene in sequence and is driven by a CAG promoter constructed from a cytomegalovirus enhancer, a chicken β -actin promoter and part of rabbit β -globin, was prepared, purified, and titrated according to the protocols supplied by the manufacturer (Takara Bio) as described (17, 18). Briefly, using the internal ribosomal entry site (IRES) fragment of the encephalomyocarditis virus, the plasmid tk-IRES-MCP1 (tk-MCP1) was constructed and the fragment was inserted into the cosmid vector (pAd-

tk-MCP1). Ad-tk-MCP1 was subsequently generated by transfecting 293 cells with pAd-tk-MCP1 and *Eco*T221-digested adenovirus 5-dix DNA-terminal protein complex. The rAd expressing HSV-tk (Ad-tk), lacZ (Ad-lacZ) and MCP-1 (Ad-MCP1) were constructed in the same way (8). The rAds were purified on cesium gradients and their titers were determined by the 50% tissue culture infectious dose (TCID₅₀) method (19).

Cell lines and culture

The human HCC cell line HuH7 (20) and the mouse HCC cell line BNL IME A.7R.1 (BNL) were cultured in DMEM (Invitrogen Life Technologies)

supplemented with 10% heat-inactivated FBS (Invitrogen Life Technologies). When infected with Ad- Δ k-MCP1 or Ad-MCP1, BNL cells produced MCP-1 protein at similar levels as HuH7 cells (data not shown), suggesting that human MCP-1 protein was efficiently expressed in the infected human and mouse HCC cell lines.

Preparation of dendritic cells (DCs) and monocytes

Murine DCs were generated using the method of Lutz et al. (21). Briefly, bone marrow cells were harvested from 6-wk-old male BALB/c-*n/n* mice (CLEA Japan). Erythrocytes were lysed with ammonium chloride potassium buffer (BioWhittaker), and the nucleated cells were placed in plastic bacteriologic dishes in 10 ml of RPMI 1640 supplemented with 10% heat-inactivated FBS and 20 ng/ml murine GM-CSF (PeproTec), with the culture medium refreshed every 3 days. On day 8, the nonadherent DCs were collected. Purity was routinely >95% CD11c⁺ DC as determined by FACS analysis.

Thioglycollate-elicited murine peritoneal exudate cells were collected as described (22). Briefly, nude mice were i.p. injected with 2 ml of 3% fluid thioglycollate medium (Wako Pure Chemical) and sacrificed 4 days later, followed by peritoneal lavage with 10 ml of cold PBS. Approximately 90% of the collected peritoneal cells were positive for both Mac-1 (CD11b) and I-A^b MHC class II when stained with PE-conjugated anti-Mac-1 Ab (clone M1/70; BD Pharmingen) and FITC-conjugated I-A^b MHC class II (clone AMS-32.1; BD Pharmingen).

Human monocytes and DCs were isolated from healthy blood donors (23). Briefly, PBMCs were isolated by centrifugation in Lymphoprep tubes (Nycomed). PBLs were then incubated in 6-well cell culture plates and the resultant adherent cells were collected as a monocyte population consisting of ~70% CD14⁺ (clone M ϕ P9; BD Pharmingen) cells, as determined by flow cytometric analysis. The monocyte population was further grown into differentiated DCs by culturing them for 1 wk in CellGro DC medium (Good Manufacturing Practice grade; Cell Genix) supplemented with 100 ng/ml GM-CSF (Cell Genix) and 50 ng/ml IL-4 (Cell Genix). The cells were collected with viability of >80%, and >60% of cells were identified as CD14⁺HLA-DR⁺ (clone L243; BD Pharmingen) DCs.

Assays for IL-12 production in vitro

HuH7 cells were infected with Ad- Δ k-MCP1, Ad- Δ k, or Ad-lacZ at a multiplicity of infection (MOI) of 5 for 24 h. Aliquots of 10⁵ DCs or monocytes were cocultured with 10⁵ rAd- or mitomycin C (MMC)-treated HuH7 cells in 1.0 ml of culture medium in a 24-well tissue culture plate and treated with or without GCV for two days at 37°C. The concentrations of IL-12 in the medium were quantitated using an immunoassay kit (BioSource International).

Animal studies

The following investigations were conducted in accordance with the Institutional Animal Care and Use Committee guidelines of Kanazawa University. Six-week-old male athymic nude mice were s.c. injected with 5 × 10⁶ HuH7 cells on day 0. On days 3 and 4, 5 × 10⁷ TCID₅₀ (100 μ l) of Ad- Δ k-MCP1, Ad- Δ k, or Ad-MCP1 was injected into the s.c. tumors, and the mice were treated with 75 mg/kg GCV injected into the peritoneal cavity every day for the next 5 days (days 5–9). Following complete eradication of the primary tumors, the mice were s.c. rechallenged on day 14 with 3 × 10⁶ HuH7 cells or injected with 1 × 10⁵ BNL cells at a distance of >3 cm from the primary challenge site. Nine of 80 (11.3%) mice treated with Ad- Δ k-MCP1 and 9 of 44 (20.4%) treated with Ad- Δ k did not show a complete eradication of the primary tumor by the final measurement and therefore were excluded from a rechallenge experiment. In some experiments, Ad- Δ k-MCP1-treated animals were i.p. administered 200 μ l of 1 mg/ml polyclonal rabbit anti-asialo GMI (AGM1) Ab (Wako Pure Chemical), an Ab against NK cells (24, 25), or 200 μ l of rabbit serum (Sigma-Aldrich), 1 ml of 2 mg/ml carrageenan (Sigma-Aldrich), which inactivates macrophages in vivo (26–28), or 1 ml of PBS on days 11, 12, 13, 20, 27, 34, 41, and 48. In another series of experiments, Ad- Δ k-MCP1-treated animals were i.p. administered 250 μ g of neutralizing goat anti-mouse IL-12 Ab (Sigma-Aldrich), 225 μ g of anti-IL-12 Ab plus 25 μ g of anti-mouse IL-18 Ab (93-10C; Medical & Biological Laboratories), or 250 μ g of control IgG Ab (goat and/or rat; Sigma-Aldrich) on days 14 and 17. Tumor sizes were measured every 4 days after the second tumor injection, and tumor volumes were calculated according to the formula (longest diameter) × (shortest diameter)²/2.

In another series of experiments, immunocompetent BALB/c-*cl* mice (CLEA Japan) were s.c. injected with 1 × 10⁵ BNL cells infected with each rAd at an in vitro MOI of 100 on day 0. GCV was administered i.p. for the next 5 days (days 1–5), and the primary tumors were completely eradi-

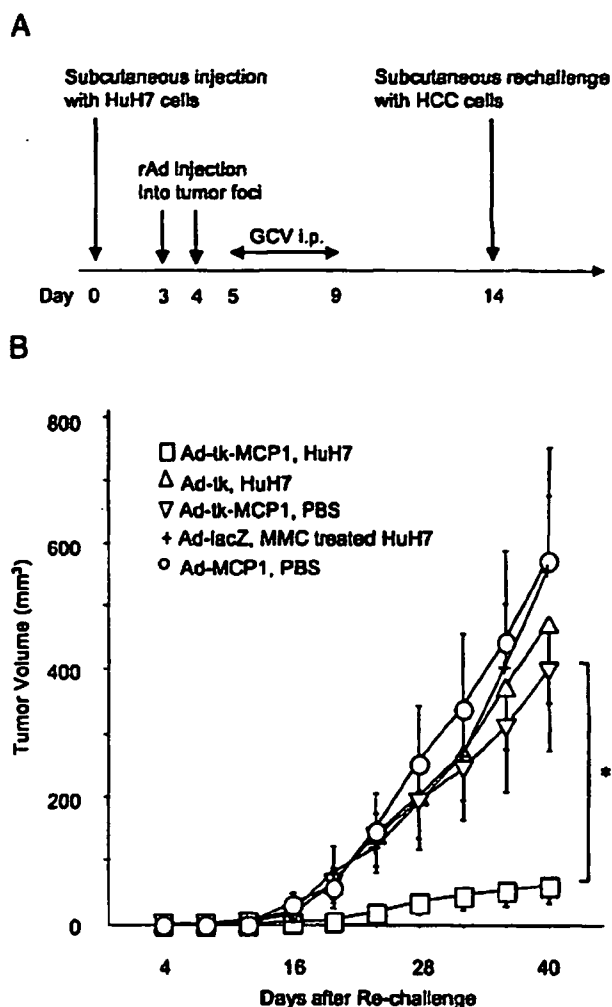


FIGURE 2. Prolonged antitumor effects of rAds expressing HSV- Δ k with or without MCP-1 in an athymic nude mouse model of HCC. **A**, Mice were s.c. injected with 5 × 10⁶ HuH7 cells on day 0. On days 3 and 4, 5 × 10⁷ TCID₅₀ of Ad- Δ k-MCP1, Ad- Δ k, Ad-lacZ, or Ad-MCP1 were injected into the tumors, and the mice were i.p. injected with 75 mg/kg GCV every day for the next 5 days (days 5–9). Following complete eradication of the primary tumors, the mice were s.c. rechallenged with 3 × 10⁶ HuH7 cells at other sites on day 14. **B**, Tumor sizes were measured every 4 days. The results are the means of three independent experiments. *, $p < 0.001$ compared to Ad- Δ k with HuH7 (Ad- Δ k, HuH7) by the Mann-Whitney's U test.

ated. These mice were s.c. injected with 1 × 10⁴ BNL cells in other sites on day 14, and the tumor sizes were measured every 7 days.

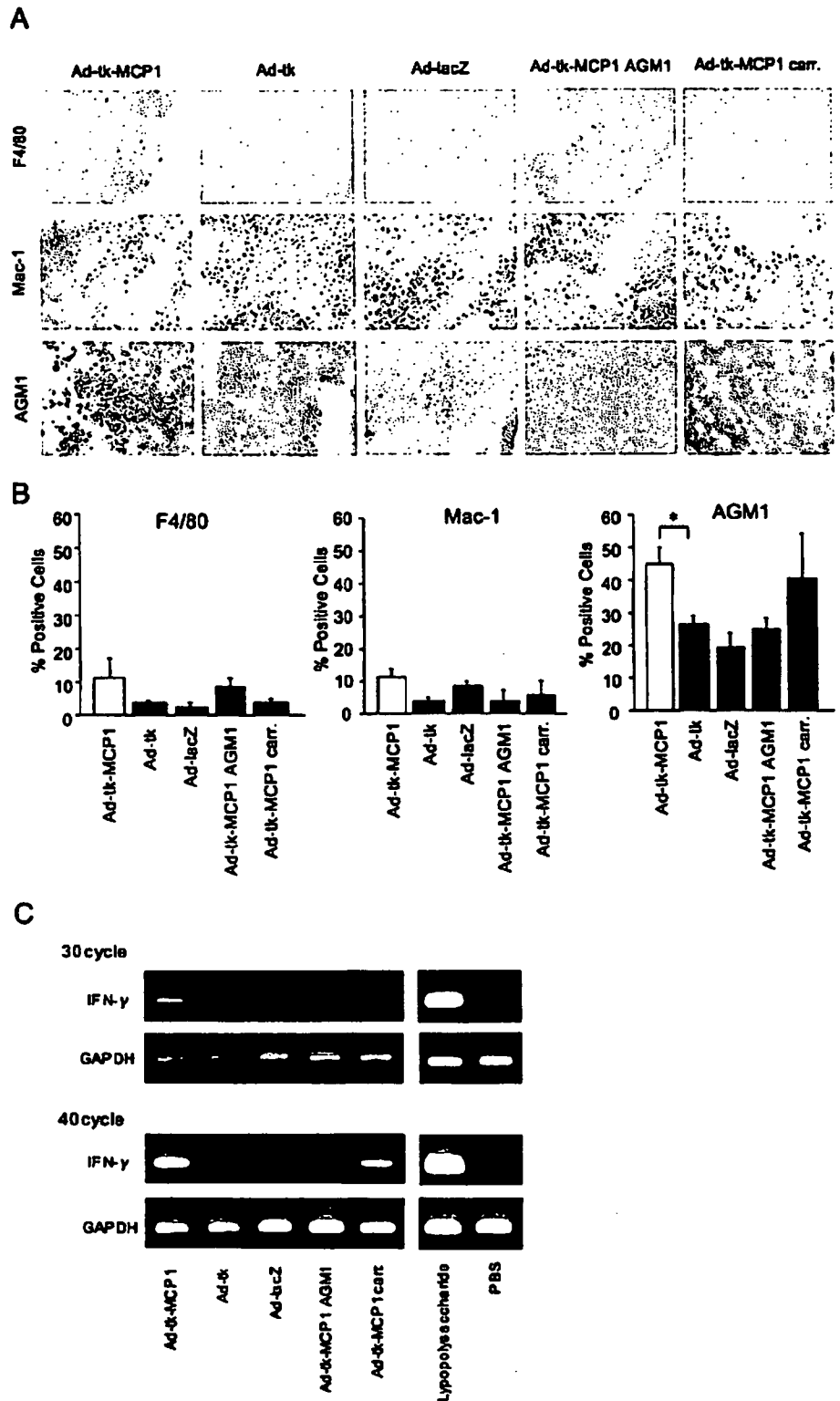
ELISA for serum IL-12 and IL-18

Mouse sera were collected before the injection of s.c. primary tumors and after the rechallenge with tumors, and IL-12 and IL-18 concentrations were measured using immunoassay kits (IL-12 from BioSource International and IL-18 from Medical & Biological Laboratories).

Immunohistochemical analysis

Tumor tissues and spleens were resected on day 16 (2 days after tumor rechallenge). The tissue samples, except those used for F4/80 (A3-1; Serotec) staining, were embedded in OCT compound (Sakura Finetek) and snap frozen in liquid nitrogen. Cryostat sections of frozen tissues were fixed in cold acetone for 10 min, followed by rinsing three times in PBS. The tissue samples used for F4/80 staining were fixed in 10% phosphate-buffered formalin and embedded in paraffin. To avoid nonspecific staining,

FIGURE 3. Expression of AGM1, F4/80, and Mac-1 Ags and IFN- γ mRNA in rechallenged tumor tissues. In the experiment described in the legend to Fig. 2, tumor tissues were resected 2 days after tumor rechallenge and analyzed immunohistochemically and estimated for IFN- γ mRNA expression by RT-PCR. **A.** Tumor tissues obtained from mice whose primary tumors were treated with Ad-ik-MCP1, Ad-ik, and Ad-LacZ, were stained with anti-AGM1, F4/80, and Mac-1 Abs. Original magnification, $\times 100$. **B.** Quantitative morphometric analysis showing the proportions of positive cells in areas of 100 tumor cells. Values are the means \pm SE of triplicate experiments. *, $p < 0.05$ compared to Ad-ik by the Mann-Whitney's U test. **C.** RT-PCR were conducted in accordance with the manufacturer's protocol as described in *Materials and Methods*. Bands corresponding to IFN- γ (384 bp) and GAPDH (265 bp) were detected. Splenocytes treated with 1 $\mu\text{g/ml}$ LPS were used as a positive marker and tumor tissues treated with PBS were used as a negative control. carr., Carrageenan.



avidin and biotin in the tissues were blocked using a blocking kit (Vector Laboratories). The slides were subsequently incubated with Abs against AGM1, F4/80, Mac-1, CD11c (HL3; BD Pharmingen), or CD45R (RA3-6B2; BD Pharmingen) for 30 min at room temperature. Negative controls included staining with the corresponding isotype for each Ab and subsequent staining with the secondary Ab. The reactions were visualized using a VECTASTAIN ABC Standard kit (Vector Laboratories), followed by counterstaining with hematoxylin.

RT-PCR for IFN- γ gene expression

Total RNA was extracted from tumor tissues resected on day 10 using a total cellular RNA isolation kit (Ambion) according to the manufacturer's protocol. Each RT-PCR was performed using 1 μg of total RNA and an oligo(dT) adaptor primer and an RNA PCR kit (avian myeloblastosis virus), version 2.1 (Takara Bio). The amplification protocol consisted of an initial denaturation at 94°C for 2 min followed by 30 or 40 cycles of

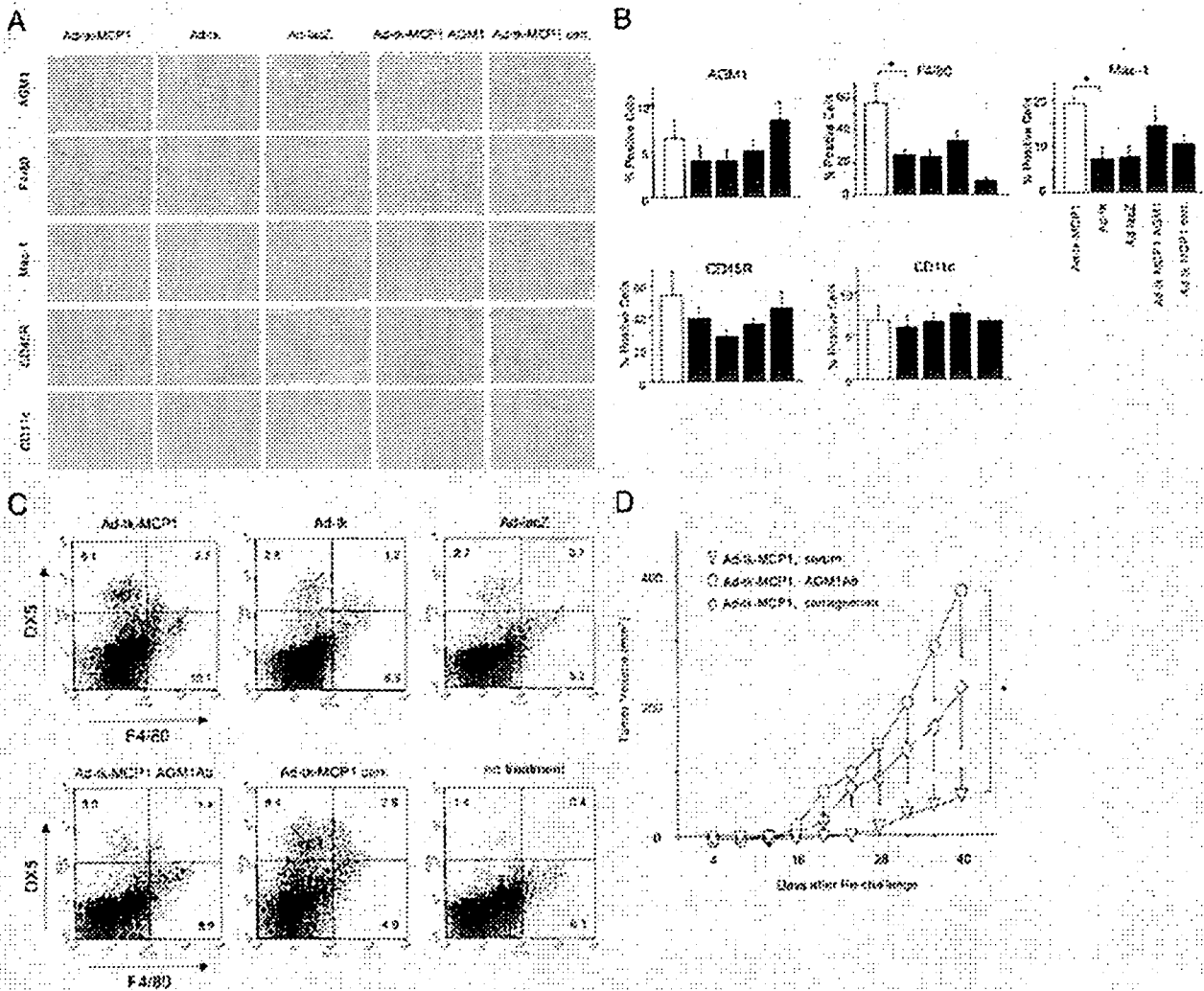


FIGURE 4. A–C. Immunohistochemical detection of AGM1, F4/80, Mac-1, CD11c, and CD45R in spleens. In the experiment described in the legend to Fig. 2, spleens were resected 2 days after the tumor rechallenge. A, The numbers of immune cells in the spleens were analyzed immunohistochemically using Ab against AGM1, F4/80, Mac-1, CD11c, and CD45R. Original magnification, $\times 100$. B, Quantitative morphometric analysis showing the percentage of positive cells in 50 \times 400 power fields. Each value is the mean \pm SE of triplicate experiments. $^* p < 0.05$ compared with Ad-ik by the Mann-Whitney *U* test. C, Surface expression of DXS and F4/80 in cell populations obtained from spleens was assessed by FACS. The results are representative of two independent experiments. carr., Carrageenan. D, The effects of anti-AGM1 Ab or carrageenan on the growth of rechallenged tumors. At the rechallenge with HuH7 cells, Ad-MCP1-treated animals were i.p. administered with 200 μ l of 1 mg/ml anti-AGM1 Ab (Ad-MCP1, AGM1 Ab), 200 μ l of rabbit serum (Ad-MCP1, serum) or 1 ml of 2 mg/ml carrageenan (Ad-MCP1, carrageenan) as described in *Materials and Methods*. Tumor sizes were measured every 4 days. The results are the means of two independent experiments. $^* p < 0.05$ compared to Ad-MCP1 with PBS or serum (Ad-MCP1, serum) by the Mann-Whitney *U* test.

denaturation at 94°C for 30 s, annealing at 60°C for 30 s, and an extension at 72°C for 1.5 min. The PCR primers for the mouse IFN- γ and GAPDH genes were purchased from R&D Systems.

Flow cytometry

Single cell suspensions of splenocytes were resuspended in PBS containing 1% BSA and 0.1% sodium azide and incubated for 30 min on ice with FITC-conjugated rat anti-mouse F4/80 and PE-conjugated rat anti-mouse pan NK cells (DXS; BD Pharmingen) or with FITC-conjugated rat anti-mouse CD4 (BD Pharmingen) and PE-conjugated rat anti-mouse CD8 (BD Pharmingen). The cells were washed, resuspended in PBS, and analyzed in a FACScan with CellQuest software.

Statistical analysis

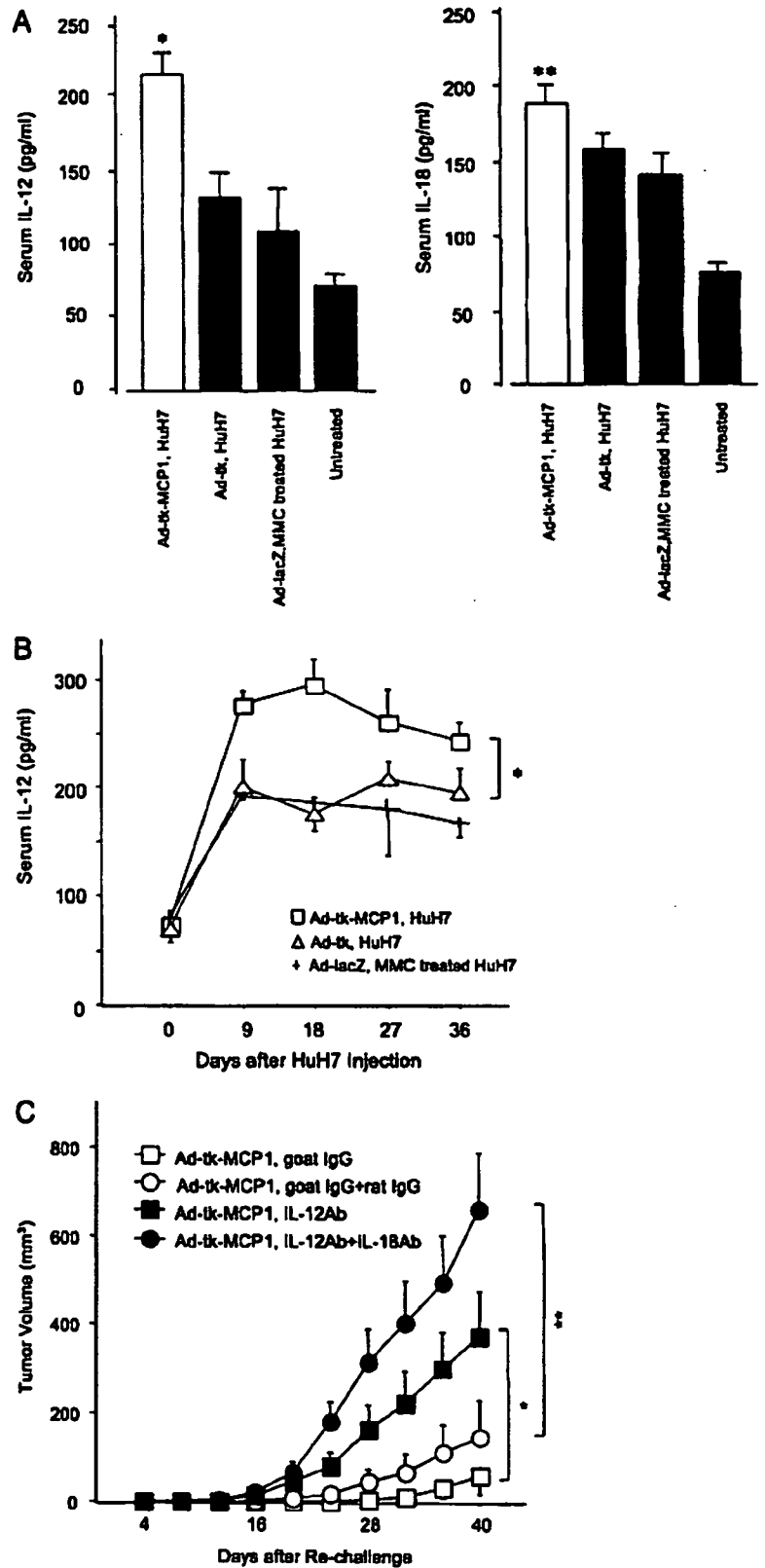
All results were expressed as means \pm SE. The statistical significance of differences between groups was evaluated by repeated measures ANOVA for the duration of the serum levels of IL-12 or the Mann-Whitney *U* test for the other results.

Results

Apoptotic HCC cells expressing MCP-1 augment IL-12 production by monocytes and DCs *in vitro*

IL-12, which was originally identified as an NK-stimulatory factor and a cytotoxic lymphocyte maturation factor, is one of the most promising cytokines in cancer treatment because of its multiple effects. IL-12 is produced by APCs such as macrophages, DCs, and B cells following the appropriate stimuli (29–31). To evaluate the immunomodulatory effects of rAds expressing HSV-tk with or without MCP-1 (Fig. 1), we measured IL-12 production by monocytes and DCs, both of which had been cocultured with HCC cells that had been infected with rAds (Fig. 1). Murine peritoneal exudate cells, consisting mostly of macrophages, and human monocytes cocultured with apoptotic HCC cells induced by the HSV-tk/GCV system plus MCP-1 produced greater amounts of IL-12

FIGURE 5. Roles of IL-12 and IL-18 in growth suppression of rechallenged HuH7 cells. **A.** Mouse sera were collected before s.c. injection of primary tumor cells (untreated) and 2 days after rechallenge with HuH7 cells, and IL-12 and IL-18 concentrations were measured using immunoassay kits. Each value is the mean \pm SE of triplicate experiments. *, $p < 0.01$; **, $p < 0.05$ compared to Ad-tk by the Mann-Whitney *U* test. **B.** Serum concentrations of IL-12 were monitored every 9 days after the injection of primary tumors. Each value is the mean \pm SE of triplicate experiments. *, $p < 0.05$ compared to Ad-tk with HuH7 (Ad-tk, HuH7) by repeated measures ANOVA. **C.** At rechallenge with HuH7 cells, Ad-tk-MCP1-treated animals were i.p. administered with 250 μ g of anti-IL-12 Ab (Ad-tk-MCP1, IL-12Ab), 225 μ g of anti-IL-12 Ab plus 25 μ g of anti-IL-18 Ab (Ad-tk-MCP1, IL-12Ab+IL-18Ab), or 250 μ g of control IgG Ab (Ad-tk-MCP1, goat IgG or Ad-tk-MCP1, goat IgG+rat IgG). Tumor sizes were measured every 4 days. The results are representative of two independent experiments. *, $p < 0.05$ compared to Ad-tk-MCP1 with goat IgG (Ad-tk-MCP1, goat IgG); **, $p < 0.01$ compared to Ad-tk-MCP1 with goat IgG plus rat IgG (Ad-tk-MCP1, goat IgG+rat IgG) by the Mann-Whitney *U* test.



than did those cocultured with apoptotic HCC cells induced by the HSV-tk/GCV system alone (Fig. 1, A and C). Murine bone marrow DCs tended to produce IL-12 when cocultured with HCC cells infected with rAds expressing MCP-1 without regard to HSV-tk-induced apoptosis (Fig. 1B). Human DCs produced

large amounts of IL-12 when cocultured with HSV-tk/GCV-induced apoptotic tumor cells, which expressed MCP-1, as did human monocytes (Fig. 1D). Thus, the phenomena observed in this xenograft model may also be observed under human allogeneic conditions.

When we measured DC maturation markers we found that their expression levels did not change when these cells were cocultured with tk/MCP-1 transduced HCC cells, whereas CD86 expression was elevated when the DCs were incubated with apoptotic HCC cells (data not shown).

Prolongation of the antitumor effects of the HSV-tk/GCV system by codelivery of the MCP-1 gene in an athymic nude mouse model of HCC

To determine the effects of HSV-tk/GCV plus MCP-1 in a murine model of HCC, HuH7 cells were s.c. transplanted into athymic nude mice and eradicated with rAds harboring HSV-tk with or without MCP-1, and the mice were rechallenged with HuH7 cells (Fig. 2A). We found that tumor regrowth was significantly lower when the primary tumor cells had been eradicated with Ad-tk-MCP1 as compared with Ad-tk (tumor volume 40 days after rechallenge, $59.2 \pm 24.9 \text{ mm}^3$ ($n = 22$) vs $471.2 \pm 118.6 \text{ mm}^3$ ($n = 20$), $p < 0.01$) (Fig. 2B). No growth inhibition was observed when Ad-tk-MCP1 or Ad-MCP1 was administered in the absence of HuH7 cell transplantation (tumor volume, $339.6 \pm 124.3 \text{ mm}^3$, $n = 18$, and $575.3 \pm 179.1 \text{ mm}^3$, $n = 12$, respectively) or when Ad-lacZ was administered along with MMC-treated HuH7 cells (tumor volume, $554.8 \pm 125.6 \text{ mm}^3$, $n = 18$). The results demonstrate that, when the primary tumors were eradicated with the HSV-tk/GCV system plus MCP-1, the antitumor effects were maintained.

Recruitment and activation of NK cells in rechallenged tumors

Serum MCP-1 concentration was below the detection limit of the ELISA used when the s.c. tumors were injected with rAds, whereas the tumor produced MCP-1 in vitro upon infection with Ad-tk-MCP-1 (data not shown). Moreover, we could not detect adenovirus DNA in these rechallenged tumors by using PCR (data not shown), negating the possibility that adenovirus infection contributed to the rejection of the rechallenged tumor. These results indicate that the injected human MCP-1 gene functioned locally in the primary s.c. tumors, thereby modulating the subsequent response to the rechallenged tumor. Because athymic nude mice possess NK cells and macrophages but not T lymphocytes, we determined the migration of these cells by an immunohistochemical analysis. The number of AGM1⁺ NK cells was significantly higher upon tumor rechallenge in mice whose primary tumors had been eradicated with Ad-tk-MCP1 plus GCV than in those whose primary tumors had been eradicated with Ad-tk plus GCV ($p < 0.05$) (Fig. 3, A and B). Similarly, the numbers of F4/80 or Mac-1 positive cells (32, 33) tended to be higher upon tumor rechallenge in mice whose primary tumors had been eradicated with Ad-tk-MCP1. Moreover, the mRNA of IFN- γ secreted by NK cells (34) became detectable after 30 PCR cycles in the rechallenged tumors of animals whose primary tumors had been eradicated with Ad-tk-MCP1 and was greatly amplified after 40 PCR cycles (Fig. 3C). These results demonstrate that NK cells were recruited and activated into rechallenged tumor tissues, presumably inhibiting tumor cell growth in mice whose primary tumors had been eradicated with HSV-tk/GCV plus MCP-1.

To monitor the activation state of innate immunity in extrahepatic lymphoid organs, we determined immunohistochemically the numbers of immune cells in the spleen after tumor rechallenge using anti-AGM1, F4/80, Mac-1, CD11c, and CD45R Abs (Fig. 4, A and B). The numbers of F4/80⁺ and Mac-1⁺ cells were significantly increased in the spleens of mice treated with Ad-tk-MCP1 compared with mice treated with Ad-tk ($p < 0.05$). In contrast, the numbers of AGM1⁺ and CD45R⁺ cells tended to be higher in the spleens of mice treated with Ad-tk-MCP1, but there was little dif-

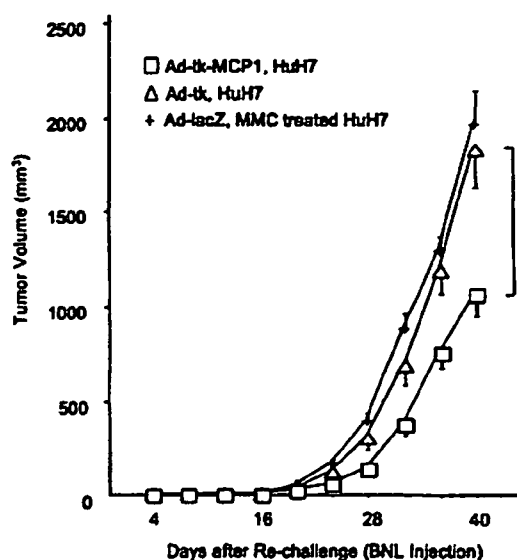


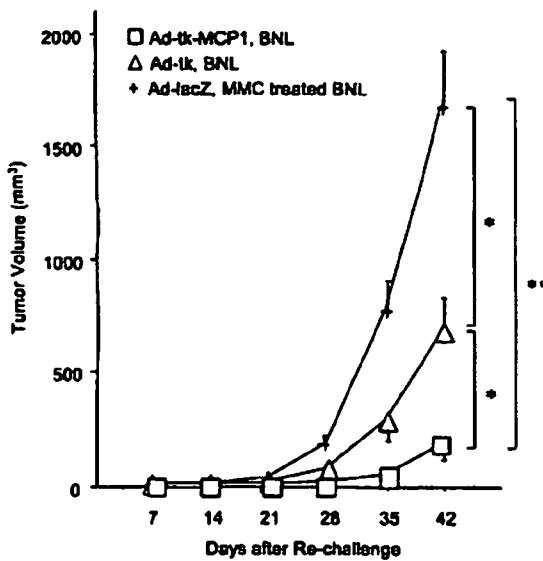
FIGURE 6. Antitumor effects of rAds expressing HSV-tk with or without MCP-1 against a second unprimed cell line (BNL) in an athymic nude mouse model of HCC. As described in the legend to Fig. 3, following complete eradication of the primary tumors the mice were s.c. injected with 1×10^3 BNL cells at other sites on day 14. Tumor sizes were measured every four days. The results are the means of two independent experiments. *, $p < 0.01$ compared to Ad-tk with HuH7 (Ad-tk, HuH7) by the Mann-Whitney's *U* test.

ference in the numbers of CD11c⁺ cells. A flow cytometrical analysis of splenocyte single cell suspensions demonstrated that the numbers of DX5⁺ and F4/80⁺ cells tended to be higher in the spleens of mice treated with Ad-tk-MCP1 (Fig. 4C). In contrast, treatment with carrageenan decreased the number of macrophages in the spleen and at rechallenge sites and slightly increased the number of NK cells in the spleen. Collectively, these results suggest that alterations in the proportions of cell subsets in splenocytes may reflect the activation status of the innate immune system following the eradication of primary tumors by HSV-tk/GCV plus MCP-1. Finally, an anti-AGM1 Ab (35, 36) significantly inhibited the antitumor immunity conferred by Ad-tk-MCP1 (tumor volume 40 days after rechallenge, $385.4 \pm 106.3 \text{ mm}^3$ ($n = 22$) vs $64.2 \pm 43.6 \text{ mm}^3$ ($n = 16$), $p < 0.05$), and carrageenan partially inhibited the antitumor immunity of Ad-tk-MCP1 (tumor volume, $242.6 \pm 100.8 \text{ mm}^3$ ($n = 14$) vs $53.8 \pm 22.9 \text{ mm}^3$ ($n = 22$), $p = 0.22$) (Fig. 4D). The results indicate that antitumor effects were mainly mediated by NK cells.

Involvement of IL-12 and IL-18 in sustained antitumor effects

IL-18 is a proinflammatory cytokine produced by activated macrophages that has been shown to augment both innate and acquired immunity (37) and, in combination with IL-12, induce Th 1 cell development and NK cell activation (38). We therefore assayed IL-12 and IL-18 production after tumor rechallenge. Serum concentrations of IL-12 and IL-18 were significantly higher after tumor rechallenge in mice whose primary tumors had been eradicated with Ad-tk-MCP1 compared with mice whose tumors had been eradicated with Ad-tk ($p < 0.05$) (Fig. 5A). Moreover, serum concentrations of IL-12 peaked after primary tumors were eradicated (day 9) and were sustained thereafter ($p < 0.05$) (Fig. 5B). Furthermore, the administration of anti-IL-12 significantly inhibited the antitumor effects conferred by Ad-tk-MCP1 (Fig. 5C) and reduced the serum concentrations of IL-12 to an undetectable level

A



B

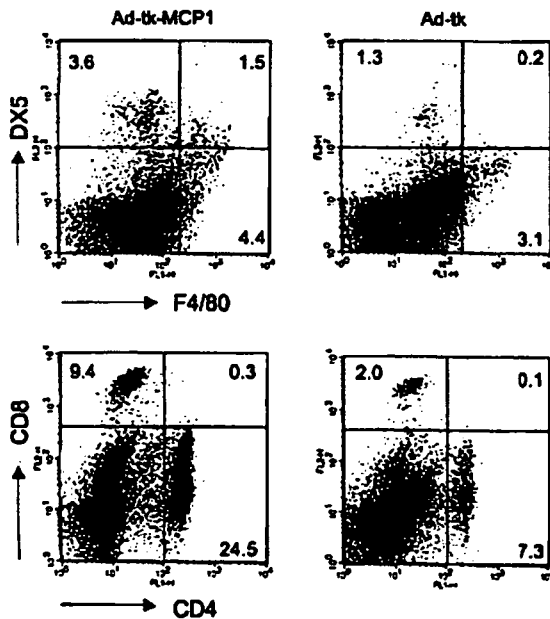


FIGURE 7. Prolonged antitumor effects of rAds expressing HSV-tk with or without MCP-1 in an immunocompetent mouse model of HCC. **A.** On day 0, mice were s.c. injected with 1×10^5 BNL cells infected with Ad-tk-MCP1, Ad-tk, or Ad-lacZ at an in vitro MOI of 100. The mice were i.p. injected with 75 mg/kg GCV per day for the next 5 days (days 1–5). Following complete eradication of the primary tumors, the mice were s.c. rechallenged with 1×10^5 BNL cells at other sites on day 14. Tumor sizes were measured every 7 days. The results are the means of three independent experiments. **, $p < 0.001$ compared to Ad-lacZ with MMC-treated BNL (Ad-lacZ, MMC treated BNL); *, $p < 0.01$ compared to Ad-tk with BNL (Ad-tk, BNL) or Ad-lacZ with MMC-treated BNL (Ad-lacZ, MMC-treated BNL) by the Mann-Whitney *U* test. **B.** Spleens were resected 70 days after the injection of primary tumor cells, and surface expression of DX5, F4/80, CD4, and CD8 in cell populations obtained from spleens was assessed by FACS. The results are representative of two independent experiments.

(data not shown). The combined treatment of anti-IL-12 and anti-IL-18 Ab further diminished antitumor effects (Fig. 5C) and reduced both serum IL-12 and IL-18 levels to undetectable levels

(data not shown). The results suggest the critical involvement of IL-12 and IL-18 in the antitumor effects induced by Ad-tk-MCP1 on tumor regrowth.

Innate immune responses to heterologous tumor injection in an athymic nude mouse

To estimate the involvement of innate immune responses in the antitumor effects observed with HSV-tk/GCV plus MCP-1, we re-challenged mice with heterologous tumor administration. The growth of a second unprimed cell line (BNL; transformed liver cells derived from BALB/c mice) was significantly suppressed when HuH7 cells had been eradicated with Ad-tk-MCP1 as compared with Ad-tk (tumor volume, $1059.5 \pm 110.6 \text{ mm}^3$ ($n = 12$) vs $1825.4 \pm 197.9 \text{ mm}^3$ ($n = 12$), $p < 0.01$) when Ad-lacZ was administered with MMC-treated HuH7 cells (tumor volume, $1960.8 \pm 183.8 \text{ mm}^3$, $n = 12$) (Fig. 6). These results indicate that the innate immune responses contributed to the prolonged antitumor effects of HSV-tk/GCV plus MCP-1 gene transfer.

Prolonged antitumor effects against mouse HCC of rAd expressing HSV-tk and MCP-1 in an immunocompetent mouse

Finally, we evaluated the antitumor responses in immune-competent mice using the same experimental procedures (Fig. 7A). The growth of rechallenged tumors was significantly lower when the primary tumor cells had been eradicated with Ad-tk-MCP1 as compared with Ad-tk (tumor volume 42 days after rechallenge, $170.3 \pm 54.2 \text{ mm}^3$ ($n = 22$) vs $488.9 \pm 120.1 \text{ mm}^3$ ($n = 22$), $p < 0.01$), similarly observed on athymic nude mice injected with human HCC. In addition, the growth of rechallenged tumors was significantly suppressed in mice whose primary tumors had been eradicated with Ad-tk as compared with those treated with Ad-lacZ and MMC ($488.9 \pm 120.1 \text{ mm}^3$ ($n = 22$) vs $1666.4 \pm 259.2 \text{ mm}^3$ ($n = 22$), $p < 0.01$). Furthermore, when we isolated splenocytes 70 days after the injection of primary tumor cells we found that the numbers of CD4⁺ and CD8⁺ cells were increased in mice treated with Ad-tk-MCP1 (Fig. 7B). Collectively, these results confirm that antitumor effects may be dependent not only on innate immunity but on acquired immune responses.

Discussion

In the current study, we observed that when monocytes were cocultured with apoptotic HCC cells infected with Ad-tk-MCP1, these immune cells produced large amounts of IL-12. Interestingly, in both nude and immunocompetent mice the growth of rechallenged HCC cells was markedly suppressed after the primary tumor cells had been eradicated with Ad-tk-MCP1 followed by GCV administration. Furthermore, these prolonged in vivo antitumor effects were associated with the production of IL-12 and IL-18 and mediated by NK cells.

Monocytes produced large amounts of IL-12 when cocultured with apoptotic HCC cells induced by the HSV-tk/GCV system plus MCP-1. APCs, such as macrophages, DCs, and B cells produce IL-12, which was originally identified as an NK-stimulatory factor and shown to exhibit considerable antineoplastic activity (39, 40). APCs were found to be activated upon the recognition of Ags from apoptotic target cells (41), and both macrophages and DCs secrete large amounts of IL-12 when treated with MCP-1 in vitro (33, 42, 43). These findings suggest that the recognition of apoptotic tumor cells together with MCP-1 may activate macrophages and DCs, thereby enhancing IL-12 secretion.

We demonstrated that the antitumor effects were maintained when the tumor cells had been eradicated with Ad-tk-MCP1, a vector that expresses both a suicide gene and a chemokine, but that either alone was not sufficient to prolong immunity in our models.

We previously demonstrated that MCP-1 secreted by apoptotic HuH7 cells may recruit and activate macrophages efficiently, although these effects did not occur when the tumor cells were treated with the rAd expressing either HSV-tk or MCP-1 (8, 10). Moreover, we observed that the numbers of Mac-1⁺ and F4/80⁺ cells were increased in the spleens of mice after tumor rechallenge. Indeed, MCP-1 has been shown to activate murine peritoneal macrophages and enhance the expression of CD11b (Mac-1) in BALB/c mice (32, 33). Collectively, these results suggest that during eradication of the primary tumors, activated macrophages in the tumor tissues and the peripheral lymphoid organs can induce the secretion of cytokines, including IL-12 and IL-18, that can activate NK cells, thus exerting antitumor effects.

IL-12-stimulated NK cells exhibit potent cytotoxic activity against various tumor cells (31, 44, 45). NK cells are a part of the innate immune system, a first-line defense against tumor cells, and exert antitumor effects of NK cells rapidly without any prior sensitization (46). The depletion of NK cells has been shown to promote metastases or tumor growth after rechallenge with primary tumor cells (15, 44, 47). We demonstrated here that the growth of rechallenged parental tumor cells or newly challenged heterologous tumor cells was suppressed after eradication of the primary tumors. Therefore, augmentation of NK-mediated innate immune responses may be an attractive strategy for preventing HCC recurrence, including the growth of differentially transformed tumor cells.

We observed that NK cell-mediated antitumor effects were prolonged after primary tumor cells had been eradicated with Ad-tk-MCP1. Several lines of evidence indicate that the inhibitory effects of NK cells on tumor growth were maintained and were detectable at the site of the primary tumor even after treatment discontinuation (36, 48). Although the mechanisms involved in these responses are not yet known, a number of tumor model systems have demonstrated the important roles of NK cells in early tumor clearance, leading to the establishment of adaptive immunity. It was recently reported that NK cell-mediated immune responses featured hallmarks of adaptive immunity such as acquired immunity, long-lived memory, and Ag specificity (16). DCs expressing IL-12 have been shown to confer NK-mediated tumor protection in which NK activation is dependent on both DC-NK interaction and IL-12 secretion (49). Moreover, NK cell-derived IFN- γ may provide early immune regulation that alters the outcome and quality of adaptive immunity (50). Furthermore, MCP-1 has been shown to induce DC migration to lesions where NK cytolytic responses are activated (51). Consistent with these observations, we demonstrated that the antitumor responses were abolished when NK cells were inactivated by treatment with the AGMI Ab and that NK cells were recruited and IFN- γ production enhanced in the rechallenged tumors.

We observed that the growth of rechallenged heterologous tumors was suppressed to a lesser extent than that of homologous tumors in our nude mice model. Athymic nude mice lack T lymphocyte-mediated immune responses, but the numbers and functions of macrophages and NK cells are preserved. Moreover, nude mice have limited populations of extrathymically matured T lymphocytes, including $\gamma\delta$ T cells (52), and these may be reduced slightly by treatment with AGMI Ab (53). Both NK cells and V δ 1 $\gamma\delta$ T lymphocytes have been reported to prevent the growth of s.c. melanoma cells, with both cell types detected at the sites of the s.c. tumors (47). Therefore, we cannot exclude the possibility that the memory subset of $\gamma\delta$ T cells affects antitumor immunity against homologous and heterologous cells, thus leading to differences in the magnitude of tumor suppression.

Although the results presented here are promising, a number of problems remain to be solved before this approach can be used clinically. First, s.c. tumor models using an HCC cell line may not be fully comparable to HCCs in patients. Second, problems using rAds need to be resolved before they can be applied clinically. However, in patients treated with nonsurgical procedures such as percutaneous radiofrequency ablation therapy and transcatheter arterial chemotherapy, the administration of rAd vectors may ensure tumor cell killing, thus enhancing the antitumor effects on residual tumor cells and recurrent HCC.

Acknowledgments

We thank Akeni Nakano and Yuzu Hasebe for assistance with histology and immunohistochemistry. We are also grateful to Maki Kawamura and Chiharu Minami for animal care.

Disclosures

The authors have no financial conflict of interest.

References

1. Venook A. P. 1994. Treatment of hepatocellular carcinoma: too many options? *J. Clin. Oncol.* 12: 1323-1334.
2. Trinchet J. C., and M. Beaugrand. 1997. Treatment of hepatocellular carcinoma in patients with cirrhosis. *J. Hepatol.* 27: 756-765.
3. Bruix J. 1997. Treatment of hepatocellular carcinoma. *Hepatology* 25: 259-262.
4. Kuriyama S., T. Sakamoto, K. Masui, T. Nakatani, K. Tominaga, M. Kikukawa, M. Yoshikawa, K. Ikenaka, H. Fukui, and T. Tsujii. 1997. Tissue-specific expression of HSV-tk gene can induce efficient antitumor effect and protective immunity to wild-type hepatocellular carcinoma. *Int. J. Cancer* 71: 470-475.
5. Kinnamlesh A. R., H. Perrin, Y. Panis, M. Fabre, H. J. Nagy, D. Houssin, and D. Klatzmann. 1997. A "distant" bystander effect of suicide gene therapy: regression of nontransduced tumors together with a distant transduced tumor. *Hum. Gene Ther.* 8: 1807-1814.
6. Okada H., K. M. Giczeman-Smits, H. Tuhara, J. Attanucci, W. K. Fellows, M. T. Lotze, W. H. Chambers, and M. E. Ilozik. 1999. Effective cytokine gene therapy against an intracranial glioma using a retrovirally transduced IL-4 plus HSVtk tumor vaccine. *Gene Ther.* 6: 219-226.
7. Hall S. J., S. E. Canfield, Y. Yan, W. Hassen, W. A. Selleck, and S. H. Chen. 2002. A novel bystander effect involving tumor cell-derived Fas and FasL interactions following Ad.HSV-tk and Ad.mIL-12 gene therapies in experimental prostate cancer. *Gene Ther.* 9: 511-517.
8. Sakai Y., S. Kaneko, Y. Nakamoto, T. Kagaya, N. Mukaida, and K. Kobayashi. 2001. Enhanced anti-tumor effects of herpes simplex virus thymidine kinase/ganciclovir system by codelivering monocyte chemoattractant protein-1 in hepatocellular carcinoma. *Cancer Gene Ther.* 8: 695-704.
9. Crittenden M., M. Gough, K. Harrington, K. Olivier, J. Thompson, and R. G. Vile. 2003. Expression of inflammatory chemokines combined with local tumor destruction enhances tumor regression and long-term immunity. *Cancer Res.* 63: 5505-5512.
10. Tsuchiyama T., S. Kaneko, Y. Nakamoto, Y. Sakai, M. Honda, N. Mukaida, and K. Kobayashi. 2003. Enhanced antitumor effects of a bicistronic adenovirus vector expressing both herpes simplex virus thymidine kinase and monocyte chemoattractant protein-1 against hepatocellular carcinoma. *Cancer Gene Ther.* 10: 260-269.
11. Allavena P., G. Bianchi, D. Zhou, J. van Damme, P. Jilek, S. Sozzani, and A. Mantovani. 1994. Induction of natural killer cell migration by monocyte chemoattractant protein-1, -2 and -3. *Eur. J. Immunol.* 24: 3233-3236.
12. Maghazachi A. A., A. al-Aoukary, and T. J. Schall. 1994. C-C chemokines induce the chemotaxis of NK and IL-2-activated NK cells. Role for G proteins. *J. Immunol.* 153: 4969-4977.
13. Loetscher P., M. Seitz, I. Clark-Lewis, M. Baggiolini, and B. Moser. 1996. Activation of NK cells by CC chemokines. Chemotaxis, Ca²⁺ mobilization, and enzyme release. *J. Immunol.* 156: 322-327.
14. Teub D. D., T. J. Sayers, C. R. Carter, and J. R. Ortaldo. 1995. Alpha and beta chemokines induce NK cell migration and enhance NK-mediated cytotoxicity. *J. Immunol.* 155: 3877-3888.
15. Nohhara H., H. Yanagawa, Y. Nishioka, S. Yano, N. Mukaida, K. Matsushima, and S. Sone. 2000. Natural killer cell-dependent suppression of systemic spread of human lung adenocarcinoma cells by monocyte chemoattractant protein-1 gene transfection in severe combined immunodeficient mice. *Cancer Res.* 60: 7002-7007.
16. O'Leary J. G., M. Goodarzi, D. L. Drayton, and U. H. von Andrian. 2006. T cell- and B cell-independent adaptive immunity mediated by natural killer cells. *Nat. Immunol.* 7: 507-516.
17. Miyake S., M. Makimura, Y. Kanegae, S. Harada, Y. Sato, K. Takamori, C. Tokuda, and I. Saito. 1996. Efficient generation of recombinant adenoviruses using adenovirus DNA-terminal protein complex and a cosmid bearing the full-length virus genome. *Proc. Natl. Acad. Sci. USA* 93: 1320-1324.

18. Sakai, Y., S. Kaneko, Y. Sato, Y. Kanegae, T. Tamaoki, I. Saito, and K. Kobayashi. 2001. Gene therapy for hepatocellular carcinoma using two recombinant adenovirus vectors with α -fetoprotein promoter and Cre/lox P system. *J. Virol. Methods* 92: 5–17.
19. Kanegae, Y., M. Makimura, and I. Saito. 1994. A simple and efficient method for purification of infectious recombinant adenovirus. *Jpn. J. Med. Sci. Biol.* 47: 157–166.
20. Nakabayashi, H., K. Taketa, T. Yamane, M. Miyazaki, K. Miyano, and J. Sato. 1984. Phenotypical stability of a human hepatoma cell line, HuH-7, in long-term culture with chemically defined medium. *Gann* 75: 151–158.
21. Lutz, M. B., N. Kukutsch, A. L. Ogilvie, S. Rossner, F. Koch, N. Romani, and G. Schuler. 1999. An advanced culture method for generating large quantities of highly pure dendritic cells from mouse bone marrow. *J. Immunol. Methods* 223: 77–92.
22. Kawaguchi, T., M. Suematsu, H. M. Koizumi, H. Mitsui, S. Suzuki, T. Matsuno, H. Ogawa, and K. Nomoto. 1983. Activation of macrophage function by intraperitoneal administration of the streptococcal antitumor agent OK-432. *Immunopharmacology* 6: 177–189.
23. Dhodapkar, M. V., R. M. Steinman, M. Sapp, H. Desai, C. Fossella, J. Krasovsky, S. M. Donahoe, P. R. Dunbar, V. Cerundolo, D. F. Nixon, and N. Bhardwaj. 1999. Rapid generation of broad T-cell immunity in humans after a single injection of mature dendritic cells. *J. Clin. Invest.* 104: 173–180.
24. Habu, S., H. Fukui, K. Shimamura, M. Kasai, Y. Nagai, K. Okumura, and N. Tamaoki. 1981. In vivo effects of anti-asialo GM1. I. Reduction of NK activity and enhancement of transplanted tumor growth in nude mice. *J. Immunol.* 127: 34–38.
25. Smyth, M. J., M. E. Wallace, S. L. Nutt, H. Yagita, D. I. Godfrey, and Y. Hayakawa. 2005. Sequential activation of NKT cells and NK cells provides effective innate immunotherapy of cancer. *J. Exp. Med.* 201: 1973–1985.
26. Ando, K., T. Moriyama, L. G. Guidotti, S. Wirth, R. D. Schreiber, H. J. Schlicht, S. N. Huang, and F. V. Chisari. 1993. Mechanisms of class I restricted immunopathology. A transgenic mouse model of fulminant hepatitis. *J. Exp. Med.* 178: 1541–1554.
27. Grosso, J. F., L. M. Herbert, J. L. Owen, and D. M. Lopez. 2004. MUC1/sec-expressing tumors are rejected in vivo by a T cell-dependent mechanism and secrete high levels of CCL2. *J. Immunol.* 173: 1721–1730.
28. Pulaski, B. A., M. J. Smyth, and S. Ostrand-Rosenberg. 2002. Interferon- γ -dependent phagocytic cells are a critical component of innate immunity against metastatic mammary carcinoma. *Cancer Res.* 62: 4406–4412.
29. Nanni, P., I. Rossi, C. De Giovanni, L. Landuzzi, G. Nicolini, A. Stoppacciaro, M. Parenza, M. P. Colombo, and P. L. Lollini. 1998. Interleukin 12 gene therapy of MHC-negative murine melanoma metastases. *Cancer Res.* 58: 1225–1230.
30. Kodama, T., K. Takeda, O. Shimozato, Y. Hayakawa, M. Aotsu, K. Kobayashi, M. Ito, H. Yagita, and K. Okumura. 1999. Perforin-dependent NK cell cytotoxicity is sufficient for anti-metastatic effect of IL-12. *Eur. J. Immunol.* 29: 1390–1396.
31. Satoh, T., T. Saika, S. Ebara, N. Kusaka, T. I. Timme, G. Yang, J. Wang, V. Mouraviev, G. Cao, E. M. A. Fattah, and T. C. Thompson. 2003. Macrophages transduced with an adenoviral vector expressing interleukin 12 suppress tumor growth and metastasis in a preclinical metastatic prostate cancer model. *Cancer Res.* 63: 7853–7860.
32. Nesbit, M., H. Schaidt, T. H. Miller, and M. Herlyn. 2001. Low-level monocyte chemoattractant protein-1 stimulation of monocytes leads to tumor formation in nontumorigenic melanoma cells. *J. Immunol.* 166: 6483–6490.
33. Biswas, S. K., and A. Sodhi. 2002. In vitro activation of murine peritoneal macrophages by monocyte chemoattractant protein-1: up-regulation of CD11b, production of proinflammatory cytokines, and the signal transduction pathway. *J. Interferon Cytokine Res.* 22: 527–538.
34. Carson, W. E., M. E. Ross, R. A. Baiocchi, M. J. Marien, N. Boiani, K. Grabstein, and M. A. Caligiuri. 1995. Endogenous production of interleukin 15 by activated human monocytes is critical for optimal production of interferon- γ by natural killer cells in vitro. *J. Clin. Invest.* 96: 2578–2582.
35. Nagai, M., and T. Masuzawa. 2001. Vaccination with MCP-1 cDNA transfectant on human malignant glioma in nude mice induces migration of monocytes and NK cells to the tumor. *Int. Immunopharmacol.* 1: 657–664.
36. van den Broeke, L. T., E. Daschtbach, E. K. Thomas, G. Andringa, and J. A. Berzofsky. 2003. Dendritic cell-induced activation of adaptive and innate antitumor immunity. *J. Immunol.* 171: 5842–5852.
37. Okamura, H., S. Kashiwamura, H. Tsutsui, T. Yoshimoto, and K. Nakanishi. 1998. Regulation of interferon- γ production by IL-12 and IL-18. *Curr. Opin. Immunol.* 10: 259–264.
38. Dinarello, C. A., D. Novick, A. J. Puren, G. Fantuzzi, L. Shapiro, H. Muhl, D. Y. Yoon, L. L. Reznikov, S. H. Kim, and M. Rubinstein. 1998. Overview of interleukin-18: more than an interferon- γ inducing factor. *J. Leukocyte Biol.* 63: 658–664.
39. Brunda, M. J., L. Luistro, R. R. Warrior, R. B. Wright, B. R. Hubbard, M. Murphy, S. F. Wolf, and M. K. Gately. 1993. Antitumor and antimetastatic activity of interleukin 12 against murine tumors. *J. Exp. Med.* 178: 1223–1230.
40. Nastala, C. L., H. D. Edington, T. G. McKimsey, H. Tahara, M. A. Nalesnik, M. J. Brunda, M. K. Gately, S. F. Wolf, R. D. Schreiber, W. J. Storkus, et al. 1994. Recombinant IL-12 administration induces tumor regression in association with IFN- γ production. *J. Immunol.* 153: 1697–1706.
41. Albert, M. L., B. Sauter, and N. Bhardwaj. 1998. Dendritic cells acquire antigen from apoptotic cells and induce class I-restricted CTLs. *Nature* 392: 86–89.
42. Matsukawa, A., C. M. Hogaboam, N. W. Lukacs, P. M. Lincoln, R. M. Strieter, and S. L. Kunkel. 2000. Endogenous MCP-1 influences systemic cytokine balance in a murine model of acute septic peritonitis. *Exp. Mol. Pathol.* 68: 77–84.
43. Traynor, T. R., A. C. Herring, M. E. Dorf, W. A. Kuziel, G. B. Toews, and G. B. Huffnagle. 2002. Differential roles of CC chemokine ligand 2/monocyte chemoattractant protein-1 and CCR2 in the development of T1 immunity. *J. Immunol.* 168: 4659–4666.
44. Lasek, W., A. Mackiewicz, A. Czajka, T. Switaj, J. Golab, M. Wizniewicz, G. Korczak-Kowalska, E. Z. Bakowicz-Iskra, K. Gryska, D. Izyski, and M. Jakobisiak. 2000. Antitumor effects of the combination therapy with TNF- α gene-modified tumor cells and interleukin 12 in a melanoma model in mice. *Cancer Gene Ther.* 7: 1581–1590.
45. Rakhmilevich, A. I., K. Janssen, Z. Hao, P. M. Sondel, and N. S. Yang. 2000. Interleukin-12 gene therapy of a weakly immunogenic mouse mammary carcinoma results in reduction of spontaneous lung metastases via a T-cell-independent mechanism. *Cancer Gene Ther.* 7: 826–838.
46. Kim, S., K. Iizuka, H. I. Agoila, I. L. Weissman, and W. M. Yokoyama. 2000. In vivo natural killer cell activities revealed by natural killer cell-deficient mice. *Proc. Natl. Acad. Sci. USA* 97: 2731–2736.
47. Orengo, A. M., E. Di Carlo, A. Comes, M. Fabbri, T. Piazza, M. Cilli, P. Musiani, and S. Ferrini. 2003. Tumor cells engineered with IL-12 and IL-15 genes induce protective antibody responses in nude mice. *J. Immunol.* 171: 569–575.
48. Lozupone, F., D. Pende, V. L. Burgio, C. Castelli, M. Spada, M. Venditti, F. Luciani, L. Lugini, C. Federici, C. Ramoni, et al. 2004. Effect of human natural killer and $\gamma\delta$ T cells on the growth of human autologous melanoma xenografts in SCID mice. *Cancer Res.* 64: 378–385.
49. Miller, G., S. Lahrs, and R. P. Dematteo. 2003. Overexpression of interleukin-12 enables dendritic cells to activate NK cells and confer systemic antitumor immunity. *FASEB J.* 17: 728–730.
50. Ortaldo, J. R., and H. A. Young. 2003. Expression of IFN- γ upon triggering of activating Ly-49D NK receptors in vitro and in vivo: costimulation with IL-12 or IL-18 overrides inhibitory receptors. *J. Immunol.* 170: 1763–1769.
51. Xu, L. L., M. K. Warren, W. L. Rose, W. Gong, and J. M. Wang. 1996. Human recombinant monocyte chemoattractant protein and other C-C chemokines bind and induce directional migration of dendritic cells in vitro. *J. Leukocyte Biol.* 60: 365–371.
52. Dandekar, A. A., and S. Perlman. 2002. Virus-induced demyelination in nude mice is mediated by $\gamma\delta$ T cells. *Am. J. Pathol.* 161: 1255–1263.
53. Geldhof, A. B., J. A. Van Ginderachter, Y. Liu, W. Noel, G. Raes, and P. De Baetselier. 2002. Antagonistic effect of NK cells on alternatively activated monocytes: a contribution of NK cells to CTL generation. *Blood* 100: 4049–4058.

Comparative proteomic and transcriptomic profiling of the human hepatocellular carcinoma

Hirotaka Minagawa ^a, Masao Honda ^{b,*}, Kenji Miyazaki ^c, Yo Tabuse ^{c,*}, Reiji Teramoto ^c, Taro Yamashita ^b, Ryuhei Nishino ^b, Hajime Takatori ^b, Teruyuki Ueda ^b, Ken'ichi Kamijo ^a, Shuichi Kaneko ^b

^a Nano Electronics Research Laboratories, NEC Corporation, 34, Miyukigaoka, Tsukuba, Ibaraki 305-8501, Japan

^b Department of Gastroenterology, Kanazawa University Graduate School of Medical Science, Kanazawa, 13-1 Takara-machi, Kanazawa 920-8641, Japan

^c Bio-IT Center, NEC Corporation, 34, Miyukigaoka, Tsukuba, Ibaraki 305-8501, Japan

Received 14 November 2007

Available online 4 December 2007

Abstract

Proteome analysis of human hepatocellular carcinoma (HCC) was done using two-dimensional difference gel electrophoresis. To gain an understanding of the molecular events accompanying HCC development, we compared the protein expression profiles of HCC and non-HCC tissue from 14 patients to the mRNA expression profiles of the same samples made from a cDNA microarray. A total of 125 proteins were identified, and the expression profiles of 93 proteins (149 spots) were compared to the mRNA expression profiles. The overall protein expression ratios correlated well with the mRNA ratios between HCC and non-HCC (Pearson's correlation coefficient: $r = 0.73$). Particularly, the HCC/non-HCC expression ratios of proteins involved in metabolic processes showed significant correlation to those of mRNA ($r = 0.9$). A considerable number of proteins were expressed as multiple spots. Among them, several proteins showed spot-to-spot differences in expression level and their expression ratios between HCC and non-HCC poorly correlated to mRNA ratios. Such multi-spotted proteins might arise as a consequence of post-translational modifications.

© 2007 Elsevier Inc. All rights reserved.

Keywords: Hepatocellular carcinoma; Proteome; Two-dimensional difference gel electrophoresis; Transcriptome; cDNA microarray

Hepatocellular carcinoma (HCC) is one of the most common cancers worldwide, and a leading cause of death in Africa and Asia [1]. Although several major risks related to HCC, such as hepatitis B and/or hepatitis C virus infection, aflatoxin B1 exposure, and alcohol consumption, and genetic defects, have been revealed [2], the molecular mechanisms leading to the initiation and progression of HCC are not well known. To find the molecular basis of hepatocarcinogenesis, comprehensive gene expression analyses have been done using many systems such as hepatoma cell lines and tissue samples [3,4]. Previously, we have carried

out a comprehensive mRNA expression analysis using the serial analysis of gene expression (SAGE) [5] and cDNA microarray-based comparative genomic hybridization [6] to acquire the outline of gene expression profile of HCC. Although these genomic approaches have yielded global gene expression profiles in HCC and identified a number of candidate genes as biomarkers useful for cancer staging, prediction of prognosis, and treatment selection [7], the molecular events accompanying HCC development are not yet understood. In general, proteins rather than transcripts are the major effectors of cellular and tissue function [8] and it is accepted that protein expression do not always correlate with mRNA expression [9,10]. Thus, protein expression analysis, which could complement the available mRNA data, is also important to understand the molecular mechanisms of HCC.

* Corresponding authors. Fax: +81 76 234 4250 (M. Honda), +81 29 856 6136 (Y. Tabuse).

E-mail addresses: mhonda@medf.m.kanazawa-u.ac.jp (M. Honda), y-tabuse@cd.jp.nec.com (Y. Tabuse).

The technique of two-dimensional difference gel electrophoresis (2D-DIGE), developed by Unlu et al. [11] is one of major advances in quantitative proteomics. Several groups have recently utilized 2D-DIGE to examine protein expression changes in HCC samples [12,13], whereas reports on the analysis combining both transcriptomic and proteomic approach are rare.

In the present study, we compared quantitatively protein expression profiles of HCC to non-HCC (non-cancerous liver) samples derived from 14 patients by 2D-DIGE. We also compared the protein expression profiles of the same HCC and non-HCC samples to the mRNA profiles which have been obtained using a cDNA microarray. The expression ratios of 93 proteins showed significant correlations with the mRNA ratios between HCC and non-HCC. Proteins involved in metabolic processes showed more prominent correlation. Our study describes an outline of gene and protein expression profiles in HCC, thus providing us a basis for better understanding of the disease.

Materials and methods

Patients. A total of 14 HCC patients who had surgical resection done in the Kanazawa University Hospital were enrolled. The clinicopathological characteristics of them are shown in Table 1. The HCC samples and adjacent non-tumor liver samples were snap frozen in liquid nitrogen, and used for cDNA microarray and 2D-DIGE analysis. All HCC and non-tumor samples were histologically diagnosed and quantitative detection of hepatitis C virus RNA by Amplicore analysis (Roche Diagnostic Systems) showed positive. The grading and staging of chronic hepatitis associated with non-tumor lesion were histologically assessed according to the method described by Desmet et al. [14] and histological typing of HCC was assessed according to Ishak et al. [15]. All strategies used for gene expression and protein expression analysis were approved by the Ethical Committee of Kanazawa University Hospital.

Preparation of cDNA microarray slides. In addition to in-house cDNA microarray slides consisting of 1080 cDNA clones as previously described [6,16–18], we made new cDNA microarray slides for detailed analysis of the signaling pathway of metabolism and enzyme function in liver disease [19]. Besides cDNA microarray analysis, a total of 256,550 tags were

obtained from hepatic SAGE libraries (derived from normal liver, CH-C, CH-C related HCC, CH-B, and CH-B related HCC), including 52,149 unique tags. Among these, 16,916 tags expressing more than two hits were selected to avoid the effect of sequencing errors in the libraries. From these candidate genes, 9614 non-redundant clones were obtained from Incyte Genomics (Incyte Corporation), Clontech (Nippon Becton Dickinson), and Invitrogen (Invitrogen). Each clone was sequence validated and PCR amplified by Dragon Genomics (Takara Bio), and the cDNA microarray slides (Liver chip 10k) were constructed using SPBIO 2000 (Hitachi Software) as described previously [6,16–18].

RNA isolation and antisense RNA amplification. Total RNA was isolated from liver biopsy samples using an RNA extraction kit (Stratagene). Aliquots of total RNA (5 µg) were subjected to amplification with antisense RNA (aRNA) using a Message Amp™ aRNA kit (Ambion) as recommended by the manufacturer. About 25 µg of aRNA was amplified from 5 µg total RNA, assuming that 500-fold amplification of mRNA was obtained. The quality and degradation of the isolated RNA were estimated after electrophoresis using an Agilent 2001 bioanalyzer. In addition, 10 µg of aRNA was used for further labeling procedures.

Hybridization on cDNA microarray slides and image analysis. As a reference for each microarray analysis, aRNA samples prepared from the normal liver tissue from one of the patients were used. Test RNA samples fluorescently labeled with cyanine (Cy) 5 and reference RNA labeled with Cy3 were used for microarray hybridization as described previously [6,16–18]. Quantitative assessment of the signals on the slides was done by scanning on a ScanArray 5000 (General Scanning) followed by image analysis using GenePix Pro 4.1 (Axon Instruments) as described previously [6,16–18].

Protein expression analysis using 2D-DIGE. Protein samples were homogenized with lysis buffer (7 M urea, 2 M thiourea, 4% w/v CHAPS, 0.8 µM aprotinin, 15 µM pepstatin, 0.1 mM PMSF, 0.5 mM EDTA, 30 mM Tris-HCl, pH 8.5) and centrifuged at 13,000 rpm for 20 min at 4 °C. The supernatants were used as protein samples. The protein concentrations were determined with a protein assay reagent (Bio-Rad). The non-HCC and HCC samples (50 µg each) labeled with either Cy3 or Cy5 according to the manufacturer's manual were combined and separated on 2-DE gels together with the Cy2-labeled internal standard (IS), which was prepared by mixing equal amounts of all samples. Analytical 2-DE was performed as described previously [20] using Immobiline DryStrip (pH 3–10, 24 cm, GE Healthcare) in the first dimension and 12.5% SDS-polyacrylamide gels (24 × 20 cm) in the second dimension. Samples were run in triplicate to obtain statistically reasonable results. After scanning with a Typhoon 9410 scanner (GE Healthcare), gels were silver stained for protein identification. For protein identification, 400 µg of the IS sample was also separately run on a 2-DE gel and stained with SYPRO Ruby (Invitrogen). All analytical and preparative gel images were processed using ImageQuant (GE Healthcare) and the protein level analysis was done with the DeCyder software (GE Healthcare). To detect phosphoproteins, 400 µg of HCC and non-HCC samples were separately run on 2-DE gels and stained with ProQ Diamond (Invitrogen). After acquiring images, gels were counterstained with SYPRO Ruby to visualize total proteins as described above.

Protein identification. The excised protein spots were in-gel digested with porcine trypsin (Promega). For LC-ESI-IT MS/MS analysis using LCQ Deca XP (Thermo Electron), the digested and dried peptides were dissolved in 10 µl of 0.1% formic acid in 2% acetonitrile (ACN). The dissolved samples were loaded onto C18 silica gel capillary columns (Magic C18, 50 × 0.2 mm), and the elution from the column was directly connected through a sprayer to an ESI-IT MS. Mobile phase A was 2% ACN containing 0.1% formic acid, and mobile phase B was 90% ACN containing 0.1% formic acid. A linear gradient from 5% to 65% of concentration B was applied to elute peptides. The ESI-IT MS was operated in positive ion mode over the range of 350–2000 (*m/z*) and the database search was carried out against the IPI Human using MASCOT (Matrix-science). The following search parameters were used: the cutting enzyme, trypsin; one missed cleavage allowed, mass tolerance window, ±1 Da, the MS/MS tolerance window, ±0.8 Da; carbamidomethyl cysteine and oxidized methionine as fixed and variable modifications, respectively.

Table 1
Characteristics of patients involved in this study

| Patient No. | Age | Sex ^a | Histology of non-tumor lesion ^b | Tumor histology | Viral status |
|-------------|-----|------------------|--|-----------------|--------------|
| 1 | 64 | M | F4A1 | Moderate | HCV |
| 2 | 65 | M | F4A1 | Well | HCV |
| 3 | 48 | M | F3A1 | Moderate | HCV |
| 4 | 69 | F | F4A2 | Moderate | HCV |
| 5 | 66 | F | F4A2 | Well | HCV |
| 6 | 45 | M | F4A1 | Well | HCV |
| 7 | 75 | F | F4A1 | Well | HCV |
| 8 | 46 | M | F4A2 | Moderate | HCV |
| 9 | 66 | M | F2A2 | Well | HCV |
| 10 | 75 | M | F3A1 | Moderate | HCV |
| 11 | 67 | F | F4A2 | Well | HCV |
| 12 | 64 | M | F4A1 | Moderate | HCV |
| 13 | 68 | M | F4A0 | Well | HCV |
| 14 | 74 | M | F1A0 | Moderate | HCV |

^a M, male; F, female.

^b F, fibrosis; A, activity.

Detection of phosphorylated peptide. Possible phosphorylation sites were investigated by MALDI-TOF-MS using monoammonium phosphate (MAP) added matrix mainly according to Nabetani et al. [21]. An additive of MAP was mixed with α -CHCA matrix solution (5 mg/mL, 0.1% TFA, 50% ACN aqueous) to 40 mM in final concentration. Trypsin digests of the spots positively stained with ProQ were dissolved into 4 μ L of 0.1% TFA, 50% ACN aqueous solution and 1 μ L of the peptides solution was spotted on the MALDI target plate. After drying up, 1 μ L of the MAP matrix was dropped on the dried peptide mixture. Voyager DE-STR (ABI) was used to obtain mass spectra both in negative and positive ion mode. MS peaks that had relatively stronger intensities in negative ion mode than in positive ion mode were selected as candidates for acidically modified peptides.

Results and discussion

We identified 195 spots representing 125 proteins (Suppl. Table 1) and obtained the corresponding mRNA expression data for a total of 93 proteins (149 spots) (Suppl. Table 2). These 93 proteins were classified according to their biological processes and subcellular localizations into categories described by the Gene Ontology Consortium (<http://www.geneontology.org/index.shtml>) and about a half of them were related to metabolic processes (Fig. 1A). It is a general agreement that proteins with extremely high or low *pI* as well as hydrophobic proteins are difficult to be detected by 2-DE. Being consistent with this notion, our analysis detected many cytoplasmic proteins (Fig. 1B). Therefore, the protein expression data presented here were biased in favor of cytoplasmic and soluble proteins. The protein expression abundance between non-HCC and HCC was calculated using the normalized spot volume, which was the ratio of spot volume relative to IS (Cy3: Cy2 or Cy5: Cy2) and we used the Student's paired *t*-test ($p < 0.05$) to select the protein spots which were expressed differentially between non-HCC and HCC, using 2-DE gel images run in triplicate. The spot volume of a multi-spotted protein was indicated as a total volume by integrating the intensities of multiple spots as was done by Gygi et al. [10]. Comparison of protein expression profiles revealed that several proteins were expressed differentially between HCC and non-HCC. Proteins whose abundances increased >2-fold or decreased <1/2 in HCC are listed in Table 2. While glutamine synthetase, vimentin,

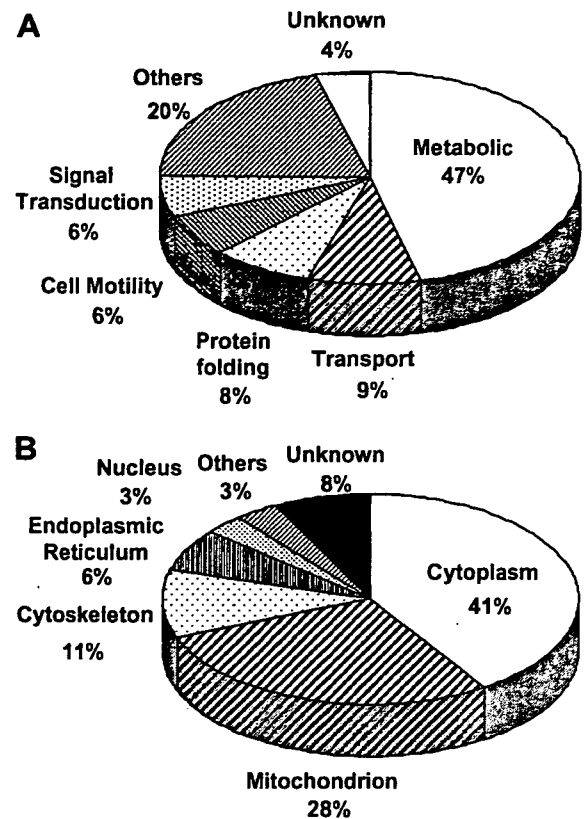


Fig. 1. Classification of identified proteins according to their cellular function (A) and subcellular localization (B).

annexin A2 and aldo-keto reductase were up-regulated, carbonic anhydrase 2, argininosuccinate synthetase 1, carbonic anhydrase 1, fructose-1,6-bisphosphatase 1, and betaine-homocysteine methyltransferase were down-regulated in HCC. Up- or down-regulation of most of these proteins in HCC has been reported previously [22–27]. Up-regulation of vimentin and annexin A2, and reduced expression of carbonic anhydrase 1 and 2 was suspected to be associated with cellular motility and metastasis [23,24,26].

The mRNA expression abundance was calculated from cDNA microarray data. Hierarchical clustering of

Table 2
Proteins expressed differentially between HCC and non-HCC

| Spot ID | Protein name | Refseq ID | Theoretical | | Fold change (HCC/non-HCC) | | References |
|------------------|--|----------------|-------------|----------|---------------------------|------|------------|
| | | | <i>pI</i> | MW (kDa) | Protein ^a | mRNA | |
| 1353, 1354 | Glutamine synthase | NP_002056.2 | 6.43 | 42.7 | 2.06 | 3.08 | [22] |
| 1039, 1046 | Vimentin | NP_003371 | 5.09 | 53.6 | 2.30 | 1.51 | [23] |
| 1716 | Annexin A2 | NP_001002857.1 | 7.57 | 38.8 | 2.57 | 1.82 | [24] |
| 1685, 1699 | Aldo-keto reductase 1B10 | NP_064695 | 7.12 | 36.2 | 4.29 | 4.73 | [25] |
| 1977 | Carbonic anhydrase 2 | NP_000058 | 6.87 | 29.3 | 0.39 | 0.62 | [26] |
| 1307, 1312, 1331 | Argininosuccinate synthetase 1 | NP_000041.2 | 8.08 | 46.8 | 0.41 | 0.30 | [27] |
| 1941 | Carbonic anhydrase 1 | NP_001729 | 6.59 | 28.9 | 0.47 | 1.25 | [26] |
| 1582 | Fructose-1,6-bisphosphatase 1 | NP_000498 | 6.54 | 37.2 | 0.48 | 0.36 | |
| 1256 | Betaine-homocysteine methyltransferase | NP_001704 | 6.41 | 45.4 | 0.48 | 0.40 | |

^a Integrated spot volume was used to calculate the fold change of multi-spotted proteins.

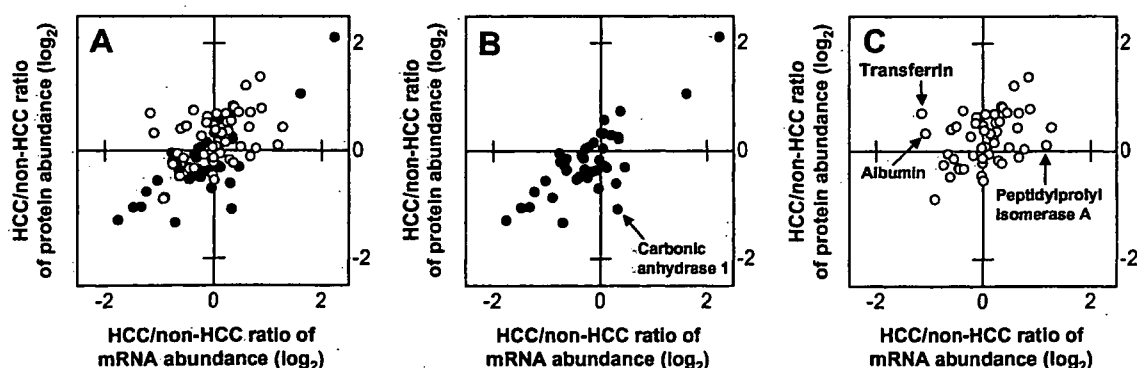


Fig. 2. Comparative analysis of protein and mRNA expression profiles between HCC and non-HCC. (A) The HCC/non-HCC ratios of averaged protein expression levels for 93 proteins were plotted against those of mRNA. Proteins related to metabolic pathways were indicated in closed circles and were shown again in (B). Proteins related to the other biochemical pathways were indicated in open circles and shown in (C). Proteins listed in Table 3 were indicated in (B) and (C). All graphs were depicted in \log_2 scale.

Table 3

Proteins whose expression changes between HCC and non-HCC show poor correlation to mRNA expression changes

| Spot ID | Protein name | Refseq ID | Theoretical | | Spot ^a Av. Ratio | Spot <i>p</i> value | Protein ratio | Micro array Av. ratio | Micro array <i>p</i> value |
|---------|----------------------------|-----------|-------------|----------|-----------------------------|---------------------|---------------|-----------------------|----------------------------|
| | | | <i>pI</i> | MW (kDa) | | | | | |
| 564 | Transferrin | NP_001054 | 6.8 | 79.3 | 2.23 | 0.035 | 1.61 | 0.45 | 3.3E-06 |
| 565 | | | | | 1.87 | 0.079 | | | |
| 566 | | | | | 2.28 | 0.13 | | | |
| 605 | | | | | 0.73 | 0.098 | | | |
| 1489 | Albumin | NP_000468 | 5.9 | 71.3 | — | 0.63 | 1.25 | 0.47 | 2.3E-03 |
| 1941 | Carbonic anhydrase 1 | NP_001729 | 6.6 | 28.9 | — | 3.5E-03 | 0.47 | 1.25 | 0.39 |
| 2290 | Peptidylprolyl isomerase A | NP_066953 | 7.7 | 18.1 | — | 5.0E-01 | 1.07 | 2.29 | 1.1E-01 |

^a Since transferrin was detected in multiple spots, averaged ratio and spot *p* value of each spot is shown.

Table 4

Multi-spotted proteins showing spot-to-spot differences in expression level between non-HCC and HCC

| Spot ID | Spot Av. ratio | Spot <i>p</i> value | Protein name | Refseq ID | Theoretical | | Protein ^a ratio |
|---------|----------------|---------------------|--------------------------------|-----------|-------------|----------|----------------------------|
| | | | | | <i>pI</i> | MW (kDa) | |
| 436 | 1.92 | 5.3E-04 | Tumor rejection antigen (gp96) | NP_003290 | 4.8 | 92.7 | 1.2 |
| 537 | 0.79 | 0.16 | | | | | |
| 564 | 2.23 | 0.035 | Transferrin | NP_001054 | 6.8 | 79.3 | 1.61 |
| 565 | 1.87 | 0.079 | | | | | |
| 566 | 2.28 | 0.13 | | | | | |
| 605 | 0.73 | 0.098 | | | | | |
| 1257 | 1.02 | 0.92 | Fumarate hydratase | NP_000134 | 8.8 | 54.8 | 0.8 |
| 1261 | 0.6 | 1.3E-03 | | | | | |

^a HCC/non-HCC protein ratios were calculated using integrated spot abundances.

gene expression was done with BRB-ArrayTools (<http://linus.nci.nih.gov/BRB-ArrayTools.htm>). The filtered data were log-transferred, normalized, centered, and applied to the average linkage clustering with centered correlation. BRB-ArrayTools contains a class comparison tool based on univariate *F* tests to find genes differentially expressed between predefined clinical groups. The permutation distribution of the *F* statistic, based on 2000 random permutations, was also used to confirm statistical

significance. A *p* value of less than 0.05 for differences in HCC/non-HCC gene expression ratio was considered significant.

The average HCC/non-HCC expression ratios of the 93 proteins were plotted against the mRNA ratios in Fig. 2, where a positive value indicates increased expression in HCC and a negative ratio indicates reduced expression. The overall expression ratio of HCC/non-HCC indicated noticeable correlation between protein and mRNA